Journal of Genetics and Genomics 47 (2020) 233–248

Contents lists available at ScienceDirect

Journal of Genetics and Genomics

Journal homepage: www.journals.elsevier.com/journal-of-genetics-and-genomics/

Original research

A functional missense variant in *ITIH3* affects protein expression and neurodevelopment and confers schizophrenia risk in the Han Chinese population

Kaiqin Li [a, b], Yifan Li [a, b], Junyang Wang [a, b], Yongxia Huo [a], Di Huang [a], Shiwu Li [a, b], Jiewei Liu [a], Xiaoyan Li [a, b], Rong Liu [a, c], Xiaogang Chen [d], Yong-Gang Yao [a, b, e, f], Ceshi Chen [a], Xiao Xiao [a], Ming Li [a, b, e, f, *], Xiong-Jian Luo [a, b, c, e, *]

[a] *Key Laboratory of Animal Models and Human Disease Mechanisms of the Chinese Academy of Sciences & Yunnan Province, Kunming Institute of Zoology, Chinese Academy of Sciences, Kunming, 650223, China*
[b] *Kunming College of Life Science, University of Chinese Academy of Sciences, Kunming, 650204, China*
[c] *Center for Excellence in Animal Evolution and Genetics, Chinese Academy of Sciences, Kunming, 650223, China*
[d] *Institute of Mental Health, National Clinical Research Center for Mental Health Disorders and National Technology Institute of Psychiatry, The Second Xiangya Hospital, Central South University, Changsha, 410011, China*
[e] *KIZ-CUHK Joint Laboratory of Bioresources and Molecular Research in Common Diseases, Kunming Institute of Zoology, Chinese Academy of Sciences, Kunming, 650223, China*
[f] *CAS Center for Excellence in Brain Science and Intelligence Technology, Chinese Academy of Sciences, Shanghai, 200031, China*

ARTICLE INFO

Article history:
Received 23 February 2020
Received in revised form
30 March 2020
Accepted 2 April 2020
Available online 6 May 2020

Keywords:
Schizophrenia
ITIH3
Missense variant
Association
Neurodevelopment
Neural stem cells

ABSTRACT

The Psychiatric Genomics Consortium (PGC) has recently identified 10 potential functional coding variants for schizophrenia. However, how these coding variants confer schizophrenia risk remains largely unknown. Here, we investigate the associations between eight potential functional coding variants identified by PGC and schizophrenia in a large Han Chinese sample ($n = 4022$ cases and 9270 controls). Among the eight tested single nucelotide polymorphisms (SNPs), rs3617 (a missense variant, p.K315Q in the *ITIH3* gene) showed genome-wide significant association with schizophrenia in the Han Chinese population ($P = 8.36 \times 10^{-16}$), with the same risk allele as in PGC. Interestingly, rs3617 is located in a genomic region that is highly evolutionarily conserved, and its schizophrenia risk allele (C allele) was associated with lower *ITIH3* mRNA and protein expression. Intriguingly, mouse neural stem cells stably overexpressing *ITIH3* with different alleles of rs3617 exhibited significant differences in proliferation, migration, and differentiation, suggesting the impact of rs3617 on neurodevelopment. Subsequent transcriptome analysis found that the differentially expressed genes in neural stem cells stably overexpressing different alleles of rs3617 were significantly enriched in schizophrenia-related pathways, including cell adhesion, synapse assembly, MAPK and PI3K-AKT pathways. Our study provides convergent lines of evidence suggesting that rs3617 in *ITIH3* likely affects protein function and neurodevelopment and thereby confers risk of schizophrenia.

Copyright © 2020, Institute of Genetics and Developmental Biology, Chinese Academy of Sciences, and Genetics Society of China. Published by Elsevier Limited and Science Press. All rights reserved.

1. Introduction

Schizophrenia (SZ) is a severe, complex, and chronic psychiatric disorder that affects ~0.5%–1% of the world's population (Saha et al., 2005). The lifetime prevalence of SZ has remained relatively high, and it was estimated that about 23.6 million people were affected by SZ in 2013 (Global Burden of Disease Study 2013 Collaborators, 2015). The clinical manifestations of SZ include positive symptoms (such as delusions and hallucinations), negative symptoms (such as impaired motivation and social withdraw), and cognitive impairments (such as poorer cognitive performance) (Owen et al., 2016). The symptoms of SZ usually begin in young adulthood (between the age of 16 and 30 years) and can last for many years. SZ also leads to substantial mortality linked with suicide (Palmer et al., 2005; Saha

* Corresponding authors.
E-mail addresses: wudaliming@163.com (M. Li), luoxiongjian@mail.kiz.ac.cn (X.-J. Luo).

https://doi.org/10.1016/j.jgg.2020.04.001
1673-8527/Copyright © 2020, Institute of Genetics and Developmental Biology, Chinese Academy of Sciences, and Genetics Society of China. Published by Elsevier Limited and Science Press. All rights reserved.

et al., 2007; Oakley et al., 2018), and patients suffer from higher comorbidity rates of other mental health problems (Buckley et al., 2009) and cardiovascular disease (Goff et al., 2005). Therefore, SZ imposes enormous burden on public well-being.

Although SZ has become a major threat to global health, currently there are few effective approaches to successfully prevent or cure this disease. A major reason for the therapeutic quandary is that we know little about the causes of SZ. To date, the etiology and pathophysiology of SZ remain largely unclear. Nevertheless, accumulating evidence suggests that both genetic and environmental factors are involved in its pathogenesis (Walker et al., 2004). The heritability of SZ was estimated to be around 0.8 (Sullivan et al., 2003), suggesting a key role of the inherited variants in the disease. To uncover the genetic basis of SZ, numerous genetic linkage and association studies have been performed and multiple candidate variants and genes were identified (Lewis et al., 2003; Allen et al., 2008; Ng et al., 2009). The advent of genome-wide association studies (GWASs) provides an unprecedented opportunity to dissect the genetic architecture of SZ. O'Donovan et al., 2008 reported the first genome-wide significant SZ risk gene *ZNF804A*. Since then, many GWASs have been conducted in different continental populations, and multiple risk variants (or loci) have been identified (Shi et al., 2011; Yue et al., 2011; Schizophrenia Working Group of the Psychiatric Genomics Consortium, 2014; Li et al., 2017; Yu et al., 2017; Pardinas et al., 2018). In 2014, the Psychiatric Genomics Consortium (PGC) identified 108 genome-wide significant SZ risk loci by analyzing 36,989 cases and 113,075 controls (Schizophrenia Working Group of the Psychiatric Genomics Consortium, 2014). For each of the reported risk loci, the PGC identified potential causal SNPs by defining a credible causal set of SNPs (the possibility that these credible causal sets of SNPs contain the true causal variants is 99%) (Schizophrenia Working Group of the Psychiatric Genomics Consortium, 2014). While most of the potential causal SNPs predicted by the PGC were located in noncoding regions, known missense variants within 10 loci were considered to be potentially causal (i.e., the reported association signal from each of these 10 loci was credibly attributable to a known nonsynonymous SNP). Clearly, these nonsynonymous SNPs can provide insights into the genetic mechanisms and pathogenesis of SZ, yet their underlying functions and mechanisms remain undefined.

To examine the roles of these 10 potential nonsynonymous polymorphisms in SZ, we performed genetic association studies and functional characterization experiments in this study. We first tested the associations between eight potential nonsynonymous SNPs identified by the PGC (rs2955365 failed to be genotyped, and rs13107325 is monomorphic in the Chinese population) and SZ in a large Han Chinese sample ($n = 4022$ cases and 9270 controls) and demonstrated that rs3617 (p.K315Q) in the ninth exon of *ITIH3* was significantly associated with SZ at the genome-wide level in the Han Chinese population. We then investigated the impact of rs3617 on *ITIH3* mRNA and protein levels, as well as proliferation, migration, and differentiation of mouse neural stem cells (mNSCs) overexpressing ITIH3 mutants with different amino acids at the rs3617 site. We further carried out transcriptome analysis to identify genes differentially expressed in mNSCs stably transfected with different alleles of rs3617. Our study provides convergent lines of evidence that supports rs3617 as a potential causal variant for SZ.

2. Results

2.1. rs3617 shows genome-wide significant association with SZ in the Han Chinese population

For each of the risk loci identified by PGC2 (Schizophrenia Working Group of the Psychiatric Genomics Consortium, 2014), the authors defined a credible causal set of SNPs. Most of the potential causal variants were in noncoding regions, except that 10 nonsynonymous SNPs were considered responsible for the association signals of these loci. We hypothesized that these nonsynonymous SNPs might also be associated with SZ in independent populations if they were causal and therefore investigated the associations between these 10 nonsynonymous SNPs and SZ in a large Han Chinese sample (4022 cases and 9270 controls). Notably, rs13107325 is monomorphic in the Han Chinese population according to 1000 Genomes data set (Abecasis et al., 2010), and rs2955365 failed to be genotyped. We thus successfully genotyped 8 nonsynonymous SNPs (Table 1). The overall genotyping call rate was 99.7%. We performed Hardy-Weinberg equilibrium (HWE) tests and found that none of the genotyped SNPs deviated from HWE in controls (Table S1). Single-site association analysis showed that the coding variant rs3617 in *ITIH3* was significantly associated with SZ in our sample ($P = 8.36 \times 10^{-16}$), even after Bonferroni correction for multiple testing (corrected $P = 6.69 \times 10^{-15}$). In addition, the SZ risk allele at rs3617 is consistent across Chinese and European populations (Pardinas et al., 2018) (Table S2), suggesting that it is likely a true risk SNP for SZ.

To further validate the association between rs3617 and SZ, we conducted a meta-analysis by combining samples from a recent study (40,675 cases and 64,643 controls) (Pardinas et al., 2018) and those of the present study. The meta-analysis (a total of 44,697 cases and 73,913 controls) showed that rs3617 was strongly associated with SZ ($P = 1.35 \times 10^{-19}$) (Table S3). Given that rs3617 is a missense variant and a potential causal variant predicted by PGC2, our validation in an independent population (i.e., Chinese sample) further supports that rs3617 is a potential causal risk variant for SZ.

2.2. rs3617 is located in an evolutionarily highly conserved region

rs3617 is located in the ninth exon (Fig. 1A) of *ITIH3*. The ITIH proteins have two conserved domains: the vault protein inter-alpha-trypsin domain and von Willebrand factor type A (vWFA) domain (Himmelfarb et al., 2004). We performed domain prediction using Prosite (https://prosite.expasy.org/) and found that rs3617 was located in the vWFA domain (Fig. 1B). By interacting with integrins, collagens, and extracellular matrix proteins, the vWFA domain plays important roles in cell adhesion (Colombatti and Bonaldo, 1991; Whittaker and Hynes, 2002). Alignment of the protein sequence from multiple vertebrate species suggests that rs3617 is in a highly conserved region (Fig. 1C), indicating vital biological roles of the proteins encoded by the sequence containing rs3617. Intriguingly, although the corresponding amino acid of the codon with rs3617 (the 315th amino acid) is lysine in most species (Fig. 1C), a different amino acid, glutamine, has emerged in humans owing to the derived allele of rs3617. We further explored whether rs3617 has an effect on the 3D structure of ITIH3 by using SWISS-MODEL (https://swissmodel.expasy.org/). The 3D structure prediction suggested that rs3617 did not exert obvious effect on the ITIH3 structure (Fig. 1D and E).

2.3. Linkage disequilibrium patterns of the 8 studied exonic SNPs in CEU and CHB populations

We compared the overall linkage disequilibrium (LD) structure across the genomic regions containing the 8 tested nonsynonymous SNPs in the main PGC population (Europeans, CEU) and Chinese population (CHB). LD comparisons mainly based on pairwise LD values between the studied exonic SNP and its surrounding variants and the LD blocks (i.e., if the exonic SNP is located in a specific LD block or in the recombination hot spot in European and Chinese populations) showed that 3 SNPs (including rs3617, rs20551 and rs3176443) had different LD

Table 1
Association significance between the eight nonsynonymous coding SNPs and schizophrenia in the Chinese population.

SNP	CHR:BP	Gene	A1/A2[a]	Amino acid change[b]	Freq_Cases[c]	Freq_Controls[d]	OR[e]	*P*
rs3176443	1:177247854	*FAM5B*	G/C	V390L	0.172	0.174	0.987	7.15E-01
rs3617	**3:52833805**	***ITIH3***	**A/C**	**K315Q**	**0.393**	**0.446**	**0.803**	**8.36E-16**
rs3774729	3:63982082	*ATXN7*	G/A	M862V	0.502	0.486	1.067	1.48E-02
rs950169	15:84706461	*ADAMTSL3*	T/C	I1660T	0.062	0.064	0.978	6.80E-01
rs4584886	17:17896205	*LRRC48*	C/T	R191W	0.126	0.129	0.971	4.68E-01
rs2288920	19:50091798	*PRRG2*	T/G	C116G	0.198	0.208	0.943	7.82E-02
rs20551	22:41548008	*EP300*	G/A	V997I	0.080	0.075	1.070	1.74E-01
rs133335	22:42416056	*WBP2NL*	A/G	D121G	0.153	0.162	0.935	6.98E-02

[a]A1/A2 represents the minor allele/major allele of each SNP. [b]Amino acid change means different alleles encode different amino acids. [c]Freq_Cases is the frequency of A1 allele in cases. [d]Freq_Controls is the frequency of A1 allele in controls. [e]OR (odds ratio) was based on A1 allele.

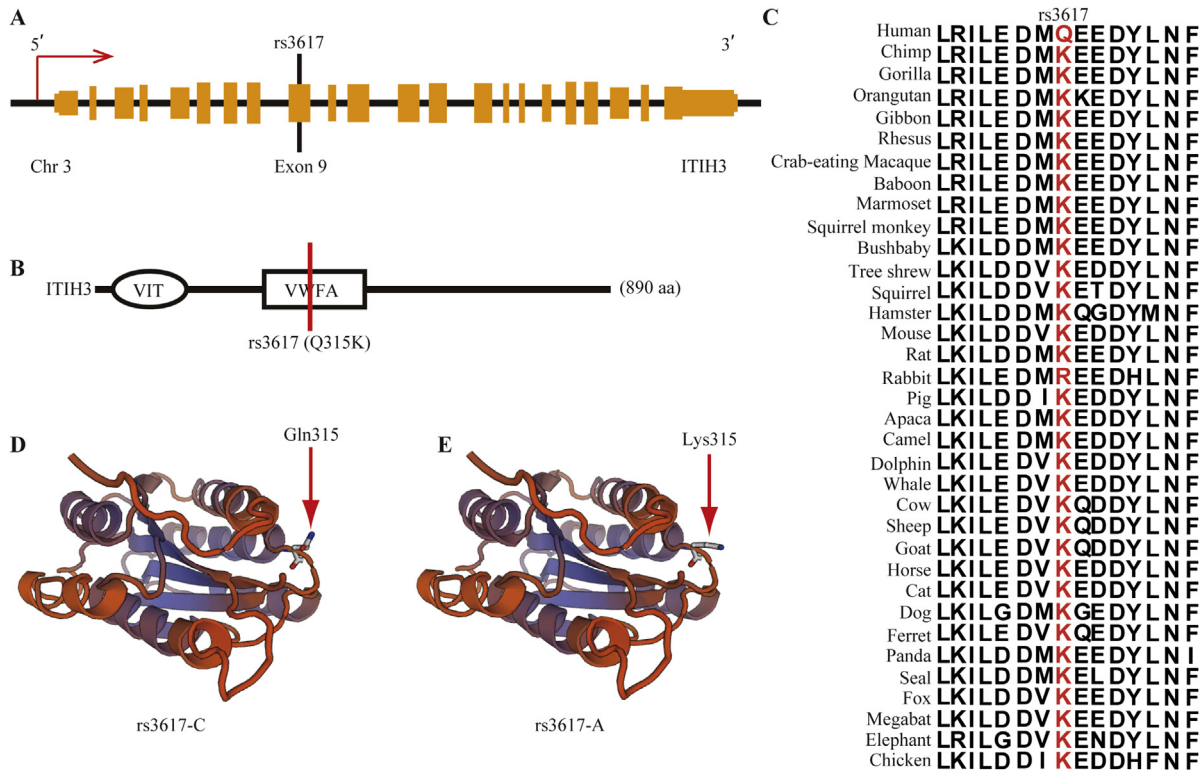

Fig. 1. rs3617 is located in an evolutionarily highly conserved region. **A**: Gene structure of *ITIH3* and the location of rs3617. Single Nucleotide Polymorphism (SNP) rs3617 is located in the exon 9 of *ITIH3* gene. **B**: SNP rs3617 is located in the vWFA domain. The C allele (risk allele) of rs3617 encodes glutamine, whereas the A allele encodes lysine. **C**: SNP rs3617 is located in an evolutionarily highly conserved region. The amino acid at the rs3617 site is lysine in most species. However, a new amino acid (glutamine) has emerged in humans. **D** and **E**: 3D structure prediction of ITIH3 protein using the SWISS-MODEL website. The locations of amino acids (lysine and glutamine) encoded by different alleles of rs3617 are shown (arrowheads). vWFA, von Willebrand factor type A; VIT, vault protein inter-alpha-trypsin.

patterns in CEU and CHB populations (Figs. S1–S3). However, the other 5 SNPs (rs4584886, rs133335, rs950169, rs2288920, and rs3774729) showed similar LD patterns in CEU and CHB populations (Figs. S4–S8).

2.4. The risk allele (C allele) of rs3617 is associated with lower ITIH3 protein and mRNA levels

Considering that rs3617 is significantly associated with SZ and located in an evolutionarily conserved region, it is possible that rs3617 affects SZ risk by modulating the pivotal biological function of ITIH3. We therefore investigated the impact of rs3617 on ITIH3 protein abundance. Expression vectors containing different alleles of rs3617 were constructed, and GFP was fused to the C-terminus of ITIH3. These expression vectors were transiently transfected into HEK293 cells, and ITIH3 protein was quantified by Western blotting after 24, 48, and 72 h from the time of transfection. We found that the SZ risk C allele consistently led to a significantly lower ITIH3 protein level at different time points after transfection compared with the A allele ($P < 0.001$, Fig. 2A–D). To further validate these results, we constructed ITIH3 expression vector by tagging Flag to the N-terminus of ITIH3. Again, we found that cells carrying the C allele had significantly lower protein levels of ITIH3 than those carrying the A allele ($P < 0.05$, Fig. 2E and F). We also explored the impact of different rs3617 alleles on ITIH3 protein levels in mNSCs stably overexpressing the gene, and consistently, the C allele of rs3617 was associated with lower ITIH3 protein expression in mNSCs (Fig. 2G and H). Theoretically, abundance of ITIH3 protein is regulated by the rates of its synthesis and degradation, and we therefore explored whether p.K315Q affects ITIH3 stability. By performing cycloheximide (CHX) chase assays (Buchanan et al., 2016), we found that the half-life of different ITIH3 isoforms (with the 315th amino acid to be either lysine or glutamine) was similar (Fig. S9), indicating that p.K315Q did not affect ITIH3 protein stability. Therefore,

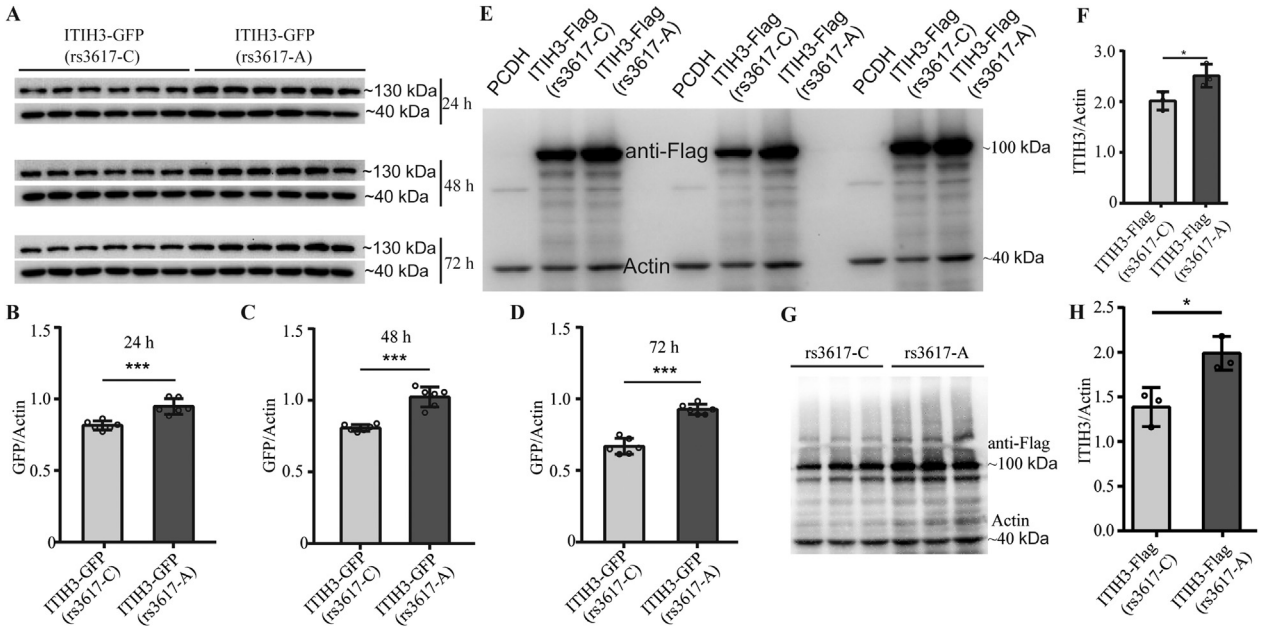

Fig. 2. The C allele of rs3617 is associated with lower ITIH3 protein expression. **A**: ITIH3 expression vectors (2.5 μg) containing C (pEGFP-*ITIH3*-C) and A (pEGFP-*ITIH3*-A allele) alleles of rs3617 were transiently transfected into HEK293 cells. Western blotting (WB) was used to quantify ITIH3 protein expression, and actin was used as an internal control. The normalized ITIH3 expression values (GFP/actin) were compared to test if different alleles of rs3617 affected ITIH3 expression. Total proteins were collected at three time points (24, 48, and 72 h) after transfection, and WB was performed. **B–D**: Quantification results of ITIH3 expression at 24 h (**B**), 48 h (**C**) and 72 h (**D**) after transfection. Data are represented as mean ± SD, and *P* values were calculated using two-tailed Student's *t*-test, $n = 6$. **E**: ITIH3 expression vectors containing different alleles of rs3617 were constructed and Flag was fused to the N-terminus of the ITIH3 coding sequence. The constructed expression vectors (2.5 μg) were transfected into HEK293 cells. Forty-eight hours after transfection, total protein was extracted, and ITIH3 expression was quantified. WB showed that the C allele of rs3617 was associated with lower ITIH3 protein expression. **F**: Quantification of the WB results shown in **E**. Data are represented as mean ± SD, and *P* values were calculated using two-tailed Student's *t*-test, $n = 3$. **G**: Proteins of mNSCs stably overexpressing different alleles of rs3617 were extracted, and WB showed that the C allele of rs3617 was associated with lower ITIH3 protein expression in mNSCs. **H**: Quantification of the WB results shown in **G**, $n = 3$. *, $P < 0.05$; ***, $P < 0.001$. SD, standard deviation; mNSC, mouse neural stem cell.

different alleles of rs3617 likely affect the synthesis of ITIH3 protein.

We also explored the effect of rs3617 on *ITIH3* mRNA expression using quantitative polymerase chain reaction (qPCR), and the results showed that rs3617 significantly affected mRNA levels of *ITIH3* (Fig. S10) in both HEK293 cells (Fig. S10A) and mNSCs (Fig. S10B). Taken together, rs3617 affects ITIH3 expression at both protein and mRNA levels.

2.5. Association between rs3617 and gene expression in the human brain

We explored the association between rs3617 and gene expression in the human brain using GTEx and LIBD data sets. rs3617 was associated with the expression of *GLYCTK*, *GNL3*, and *PPM1M* in GTEx (Table S4). In the LIBD data set, rs3617 was associated with the expression of *GNL3* ($P = 7.89 \times 10^{-11}$) and *NEK4* ($P = 1.89 \times 10^{-6}$) (Table S5). No significant association between rs3617 and *ITIH3* expression was observed in either data set. We noticed that mRNA levels of *ITIH3* were relatively low in human brain tissues (Fig. S11), which may explain why no significant association between rs3617 and *ITIH3* expression was observed in brain expression quantitative trait loci (eQTL) data sets. In addition, considering the high LD between rs3617 and other genetic variants (Fig. S12), it is also possible that the associations between rs3617 and other genes resulted from the signals of its LD SNPs.

2.6. The C allele of rs3617 promotes the proliferation of mNSCs compared with the A allele

The neurodevelopmental hypothesis of SZ posits that SZ originates from abnormal brain development (Owen et al., 2011) and has gained support from accumulating evidence. For example, Walsh et al., 2008 found that gene-disrupting rare structural variants identified in SZ cases were enriched in neurodevelopmental pathways. Functional studies of SZ risk genes (such as *DISC1* and *RELN*) also further confirmed the involvement of abnormal neurodevelopment in the disease (Mao et al., 2009; Ishizuka et al., 2011; Senturk et al., 2011). We showed that the risk allele of rs3617 was associated with lower ITIH3 expression. To further explore the potential functional consequence of rs3617, we investigated the effect of rs3617 on neurodevelopment. We isolated the mNSCs from embryonic brains (E13.5) as previously described (Yang et al., 2018) and confirmed that mNSCs were successfully isolated and purified by immunofluorescence co-labeling of the well-characterized NSC markers (including SOX2, NESTIN, and PAX6) (Fig. 3A–E). We transfected the mNSCs with ITIH3 expression vectors (carrying different alleles at rs3617) to generate mNSCs stably overexpressing ITIH3. Proliferation of these cells was then evaluated by 5-bromo-2-deoxyuridine (BrdU) incorporation experiments. Intriguingly, mNSCs carrying the SZ risk C allele at rs3617 exhibited significantly higher proliferation rates than those carrying the nonrisk A allele ($P < 0.001$, Fig. 3F and G). Further cell proliferation experiments using Cell Counting Kit-8 (CCK-8) also showed consistent results ($P < 0.01$, Fig. 3H), which determines cell viability through reduction reaction (WST-8 is reduced by dehydrogenases, and the amount of the reduction products [formazan] is directly proportional to the number of living cells). We have also transiently transfected ITIH3 expression vectors into HEK293 cells and tested the effects of different alleles at rs3617 on cell proliferation after 48 h. Again, both BrdU and CCK-8 assays suggested that transfection of vectors carrying the C allele at rs3617 resulted in significant increase of the cell proliferation rate (Fig. 3I–K). Taken together, rs3617 likely affects neurodevelopment by modulating NSC proliferation.

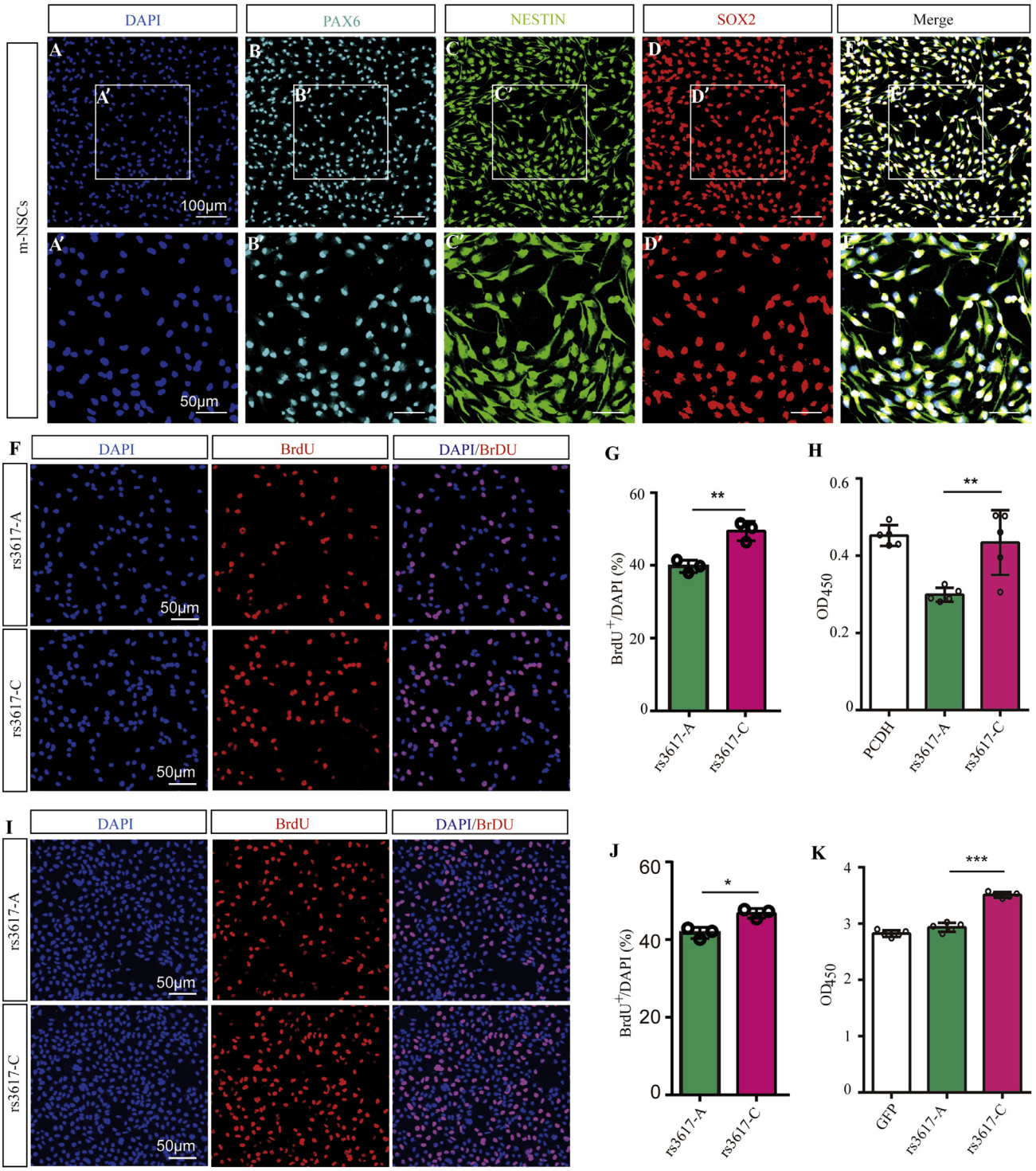

Fig. 3. The mNSCs stably transfected with different alleles of rs3617 exhibited significant differences in proliferation. **A**–**E**: Isolation and characterization of the mNSCs. Immunofluorescence staining with three well-characterized NSC markers (PAX6, NESTIN, and SOX2) confirmed that the cells isolated were NSCs. **F**: BrdU incorporation assay showed that NSCs stably transfected with the rs3617 C allele had significantly higher proliferation rates than those transfected with the rs3617 A allele. **G**: The quantified results of the BrdU incorporation assay. **H**: CCK-8 assay revealed that NSCs stably transfected with the C allele had higher proliferation rates. **I**: HEK293 cells transiently transfected with the C allele had significantly higher proliferation rates than cells transfected with the A allele. **J**: Quantified results of the BrdU incorporation assay in **I**. **K**: CCK-8 assay revealed that HEK293 cells transiently transfected with ITIH3 expression vector containing the C allele of rs3617 had higher proliferation rates than cells containing the A allele. Data are represented as mean ± SD, and *P* values are calculated using two-tailed Student's *t*-test; $n = 3$ and a total of 10 randomly selected immunostaining images were used for cell counting for **G**; $n = 5$ for **H**; $n = 3$ and a total of six immunostaining images were used for cell counting for **J**; $n = 5$ for **K**. *, $P < 0.05$; **, $P < 0.01$; ***, $P < 0.001$. mNSC, mouse neural stem cell; SD, standard deviation; BrdU, 5-bromo-2-deoxyuridine; CCK-8, Cell Counting Kit-8.

2.7. The C allele of rs3617 inhibits the migration of mNSCs compared with the A allele

We further investigated the effects of C and A alleles of rs3617 on migration of mNSCs. The cells were isolated and stably transfected with vectors carrying either the C or A allele at rs3617 and then cultured in a proliferation medium to generate neurospheres. Neurospheres with similar diameters were seeded into laminin-precoated plates and cultured in a differentiation medium for 24 h. The migration distances of the seeded neurospheres were then measured. We found that the migration distances of mNSCs stably overexpressing the SZ risk C allele at rs3617 were significantly shorter than those stably overexpressing the A allele ($P < 0.05$) (Fig. 4). Therefore, rs3617 might also affect neurodevelopment by modulating NSC migration.

2.8. rs3617 affects the differentiation of mNSCs

Neural differentiation, an essential process in neurodevelopment, has also been found to be affected by SZ risk genes (Yang et al., 2018; Chen et al., 2018). We therefore also explored whether different alleles of rs3617 exerted different impacts on neural differentiation. In brief, mNSCs stably transfected with either the C or A allele of rs3617 were differentiated into neurons and glial cells and stained for the neuronal markers (TUJ1 and MAP2) and the glial marker (GFAP). The ratio of GFAP (a marker for glial cells), MAP2 (a marker for mature neurons) and TUJ1 (a marker for newly generated immature postmitotic neurons)-positive cells was calculated and compared to reveal the differentiation ability of mNSCs carrying different alleles at rs3617. Indeed, significantly different differentiation capabilities were seen in cells with different genotypes at rs3617 (Fig. 5). Compared with mNSCs stably transfected with the A allele of rs3716, the differentiation of mNSCs with the C allele into astrocytes (marked with GFAP, a marker for astrocytes) was significantly impaired ($P < 0.001$) (Fig. 5A and B). By contrast, significant increases in the ratios of MAP2 (Fig. 5C and D) and TUJ1 (Fig. 5E and F) positive cells were observed in mNSCs carrying the C allele compared with those stably transfected with the A allele. These results confirmed the allelic effects of rs3617 on neural differentiation (i.e., the ratios of glial and neuronal cells).

2.9. rs3617 does not affect ITIH3 protein localization

We then examined if different amino acids resulted from rs3617 affected ITIH3 protein localization. However, immunofluorescence showed that rs3617 did not affect the subcellular localization of ITIH3 in either HEK293 cells (Fig. S13) or mNSCs (Fig. S14). Therefore, rs3617 likely affected ITIH3 through mechanisms other than altering protein localization. In addition, to exclude the potential influences of endogenous ITIH3 on our results, we performed real-time qPCR (RT-qPCR) and confirmed that no obvious endogenous *ITIH3* expression was detected in HEK293 cells (Fig. S15A). In mNSCs, *Itih3* expression was also very low as evaluated by both RT-qPCR (Fig. S15B) and RNA sequencing (RNA-Seq). Specifically, the average expression value (counts from RNA-Seq data) of the well-characterized NSC marker *Sox2* was 43,283 in mNSCs, whereas that of *Itih3* was only 95. Taken together, endogenous *ITIH3* should not affect our results significantly.

2.10. Dosage-dependent effect of ITIH3 on proliferation

Although the effect of rs3617 on cell proliferation was convincing, it was not clear whether this effect was attributed to the altered expression of the ITIH3 protein expression level as the constructs of different rs3617 alleles might differ in their activities and thereby confound the results. We therefore conducted a dosage-dependent assay and confirmed that the ITIH3 expression level was proportional to the amount of vectors transfected with the C allele of rs3617 (Fig. S16A). Interestingly, we found that the proliferation rate of HEK293 cells was decreased as the transfected amount of ITIH3 expression vector increased (Fig. S16B). These data are consistent with the results presented in Fig. 3, suggesting that the observed proliferation difference was likely due to the altered ITIH3 protein levels. Nevertheless, whether rs3617 affects the activity of ITIH3 remains to be defined.

2.11. rs3617 regulates SZ-related biological pathways

Our aforementioned data suggest that rs3617 confers SZ risk by affecting *ITIH3* function and neurodevelopment. To further investigate the potential mechanisms underlying these functional impacts of rs3617, RNA-Seq and subsequent qPCR validation were carried out. We identified 669 genes that were differentially expressed between mNSCs stably transfected with the C allele of rs3617 and those carrying the A allele (Fig. 6A). The top 30 most significantly altered genes are shown in Fig. 6B. Five genes (including *Peg10*, *Sgce*, *Dbx2*, *Rasgrp3*, and *Syt1*) were selected from these top 30 genes for qPCR validation (Fig. 6B) as their pivotal roles in the brain have been consistently reported before. For example,

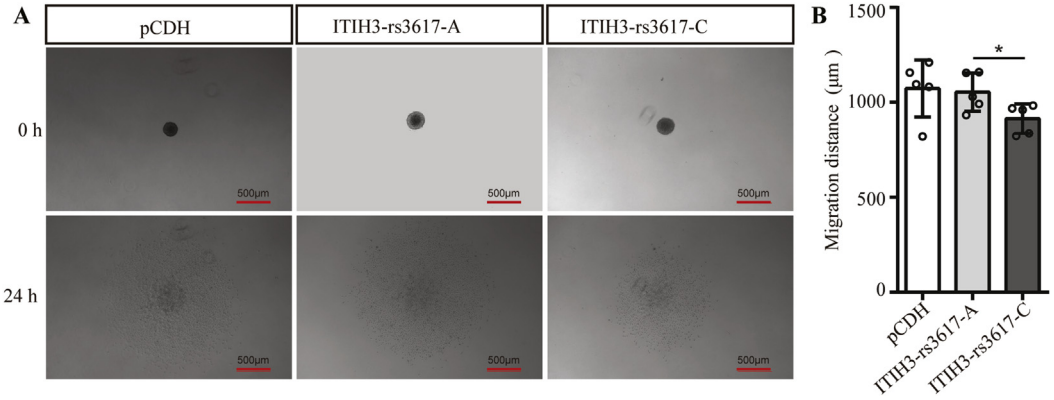

Fig. 4. NSCs stably transfected with different alleles of rs3617 exhibited significant differences in migration. **A**: Representative photographs for the migration assay. Neurospheres with similar diameters were selected and seeded into laminin-coated 24-well plates. After culturing neurospheres in the differentiation medium for 24 h, the migration distances of neurospheres were measured by subtracting the radius of the original neurosphere from the radius of the neurosphere at 24 h. **B**: Quantified results of the migration assay in **A**. Data are represented as mean ± SD, and *P* value was calculated using two-tailed Student's *t*-test; 5 independent neurospheres were analyzed for each group. Scale bar represents 500 μm in **A**. *, $P < 0.05$. NSC, neural stem cell; SD, standard deviation.

Dbx2 is involved in neurogenesis, and *Syt1* has a role in maintaining the function of synapses (Ullrich et al., 1994; Ma et al., 2011). *SGCE* mutations are associated with psychiatric disorders (Peall et al., 2015), and *Rasgrp3* is involved in cell migration (Randhawa et al., 2011). Consistent with the RNA-Seq results, qPCR showed that *Peg10*, *Sgce*, and *Dbx2* were significantly downregulated in mNSCs stably transfected with the C allele of rs3617 compared with those transfected with the A allele (Fig. 6C–E); whereas *Rasgrp3* and *Syt1* were significantly upregulated in mNSCs carrying the C allele at rs3617 (Fig. 6F and G). We then performed Gene Ontology (GO) analysis and found that the differentially expressed genes were significantly enriched in cell adhesion, synapse organization, positive regulation of cell migration, gliogenesis, and synapse assembly pathways (Fig. 6H). Intriguingly, cell adhesion (Kirov et al., 2009; Liu et al., 2018), synapse function (Fromer et al., 2014), cell migration (Senturk et al., 2011; Ishii et al., 2016), and gliogenesis (Windrem et al., 2017)) have all been highlighted in SZ studies. Therefore, rs3617 may participate in SZ pathogenesis *via* modulating these pathways.

We also performed Kyoto Encyclopedia of Genes and Genomes (KEGG) analysis and found that the differentially expressed genes were significantly enriched in MAPK, extracellular matrix (ECM)-receptor interaction, adhesion, and PI3K-AKT signaling pathways (Fig. 6I). Intriguingly, the *ITIH3* gene encodes the heavy-chain subunit of the pre-alpha-trypsin inhibitor complex, which binds hyaluronic acid and thereby stabilizes the extracellular matrix. Therefore, our results and previous studies provide convergent evidence that alterations in extracellular matrix function might mediate the biological impact of rs3617 in SZ pathogenesis. In addition, previous studies have revealed pivotal roles of MAPK and PI3K-AKT signaling pathways in SZ (Emamian et al., 2004; Funk et al., 2012). It is thus highly likely that rs3617 may contribute to SZ by regulating these signaling pathways. Based on the aforementioned findings, we proposed a possible hypothesis to elucidate the potential role of rs3617 in SZ pathogenesis (i.e., rs3617 may confer SZ risk by affecting the ITIH3 protein level and neurodevelopment) (Fig. 7).

3. Discussion

GWASs of SZ have identified more than 180 risk loci showing strong associations with SZ (Schizophrenia Working Group of the Psychiatric Genomics Consortium, 2014; Li et al., 2017; Pardinas et al., 2018). However, the causal variants and genes remain largely unknown for most of the reported risk loci. Considering that most of the identified risk variants were located in noncoding regions, it is likely that a large proportion of risk variants exert their effects on SZ by modulating gene expression (rather than affecting protein function). Accordingly, recent studies have mainly focused on noncoding risk variants (Luo et al., 2015; Yang et al., 2018), leaving the coding variants, which likely participate in an illness by altering the protein structure and function, relatively less investigated in SZ (Li et al., 2016). In this study, by exploring the associations between the potential causal coding variants and SZ in a large Han Chinese sample, we showed that a nonsynonymous SNP in the *ITIH3* gene, rs3617, was significantly associated with the disease and therefore was likely an authentic risk variant for SZ.

The successful replication of rs3617 in the Han Chinese population provides further evidence that supports its involvement in SZ. Interestingly, rs3617 has the same risk allele (i.e., C allele) in European and Chinese populations, indicating that it is a common risk variant in different ethnic populations. We have also explored the impact of different alleles of rs3617 on *ITIH3* function. We show that rs3617 is located in an evolutionarily highly conserved region, and its SZ risk C allele is associated with lower ITIH3 protein expression. Intriguingly, mNSCs stably transfected with different alleles of rs3617 exhibited significant differences in proliferation, differentiation, and migration, suggesting that rs3617 may exert its biological effect by modulating neurodevelopment. Transcriptome analysis using mNSCs stably transfected with different alleles of rs3617 has identified potential biological processes (or pathways) affected by rs3617. Specifically, genes differentially expressed between cells with different alleles at rs3617 are enriched in cell adhesion, synapse organization, and cell migration processes, confirming the potential impact of rs3617 on neural migration and neurodevelopment. These results provide convergent evidence that rs3617 is likely a causal variant that confers SZ risk by affecting neurodevelopment.

Although the PGC predicted that rs3617 might be a potential causal variant, to date, the functional consequences and biological effects of rs3617 remain elusive. In this study, we provide convergent lines of evidence that support rs3617 as a causal variant for SZ. First, rs3617 is located in the coding region of *ITIH3* and does cause altered amino acid sequences of ITIH3. Second, rs3617 is also associated with SZ in the Han Chinese population, further supporting its putative role in SZ. Third, the genomic region harboring rs3617 is highly evolutionarily conserved, suggesting the functional conservation of this genomic region. Fourth, the allelic differences at rs3617 lead to amino acid change from lysine (corresponding to the A allele) to glutamine (corresponding to the C allele). Considering that lysine and glutamine have different physiochemical properties (for example, lysine is a charged amino acid, whereas glutamine is uncharged), the differences of the amino acid at rs3617 may affect ITIH3 function. Fifth, we show that the C allele of rs3617 is associated with lower ITIH3 protein expression. Sixth, mNSCs stably transfected with different alleles of rs3617 exhibit significant differences in proliferation, migration, and differentiation, confirming the functional consequences of rs3617. Seventh, the differentially expressed genes identified in mNSCs stably transfected with different alleles of rs3617 are significantly enriched in MAPK, cell adhesion, and PI3K-ATK signaling pathways. Considering the pivotal role of these signaling pathways in SZ (Emamian et al., 2004; Funk et al., 2012), it is possible that rs3617 confers SZ risk by modulating these signaling pathways. Taken together, these convergent lines of evidence suggest that rs3617 is a causal variant for SZ.

Accumulating evidence supports that *ITIH3* is likely an authentic risk gene for psychiatric disorders. Genetic variants near *ITIH3* have been reported to be associated with SZ (Schizophrenia Psychiatric Genome-Wide Association Study (GWAS) Consortium, 2011; Yang et al., 2019), bipolar disorder (Psychiatric GWAS Consortium Bipolar Disorder Working Group, 2011), and depression (Miyake et al., 2018). In addition to the significant associations observed in European populations, Li et al. (2015) also found that a SNP (rs2239547) near the *ITIH3/4* locus was significantly associated with SZ in the Han Chinese population. In line with the genetic studies, a recent study showed that functional deficiency of *Itih3* in mice led to abnormal behaviors, including increased anxiety-like behavior, reduced exploratory activity, altered acoustic startle responses, and so on (Goulding et al., 2019). These behavioral results provide further support for the involvement of *ITIH3* in psychiatric disorders.

ITIH3 is a member of the inter-alpha-trypsin inhibitor (ITI) family. *ITIH3* encodes ITI heavy chain H3, a subunit of the pre-alpha-trypsin inhibitor complex (Diarra-Mehrpour et al., 1998). Previous studies have shown that the pre-alpha-trypsin inhibitor complex is involved in extracellular matrix stabilization (Bost et al., 1998; Diarra-Mehrpour et al., 1998). The extracellular matrix has important functions in the developing brain. It is involved in differentiation of NSCs, neuronal migration, the formation of axonal tracts, and the maturation of synapses in the brain (Barros et al.,

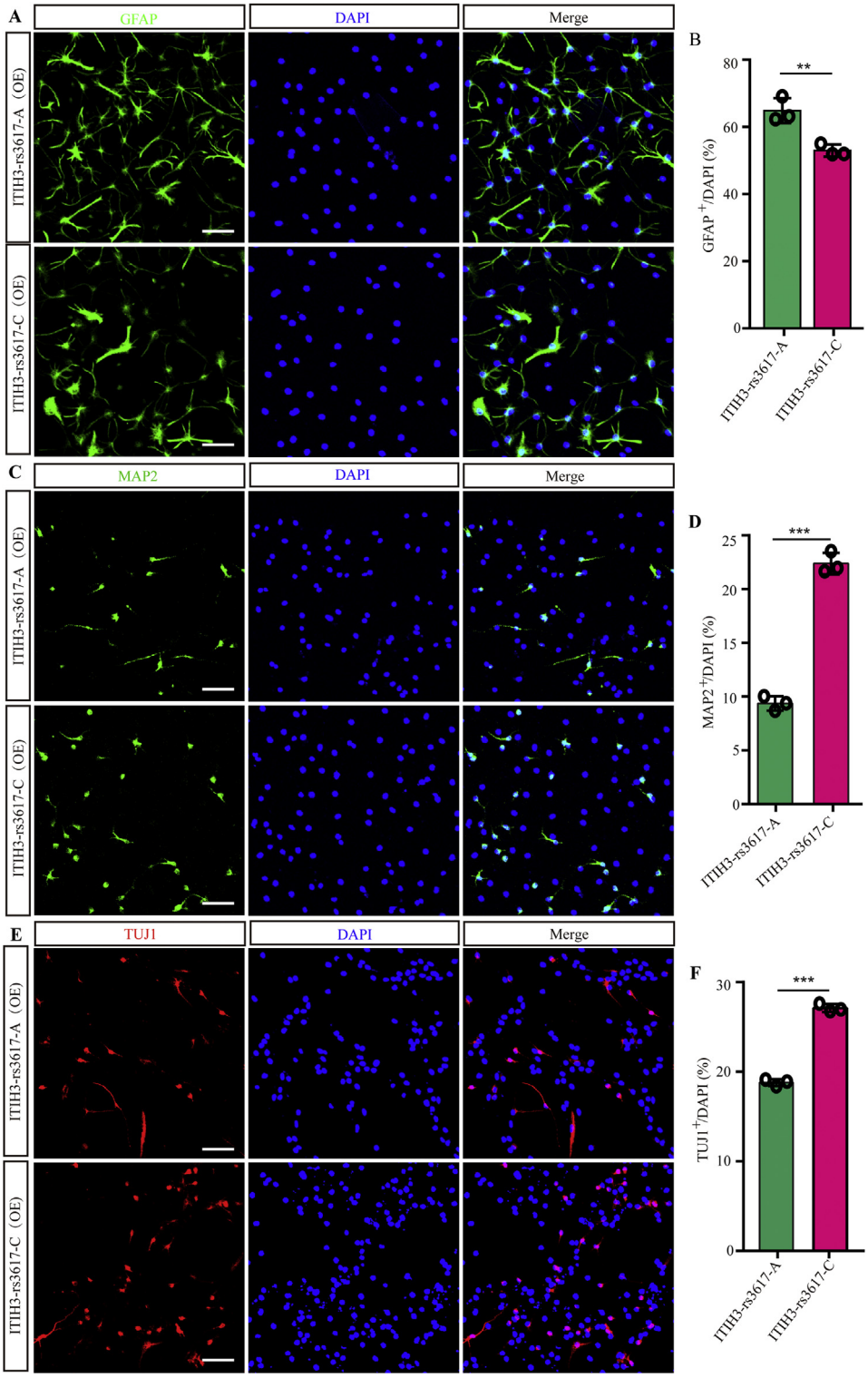

Fig. 5. The mNSCs stably transfected with different alleles of rs3617 exhibited significant differences in differentiation. **A**: Differentiation of mNSCs stably transfected with either the C or A allele of rs3617 into astrocytes. Representative immunostaining for GFAP, a marker for astrocytes. **B**: The quantification of results in **A**. Compared with mNSCs stably transfected with the A allele of rs3716, the differentiation of cells stably transfected with the rs3617 C allele into astrocytes (GFAP-positive) was significantly impaired. **C**: Differentiation of mNSCs into mature neurons. Representative immunostaining images for MAP2, a marker for mature neurons. **D**: The quantified results in **C**. Compared with mNSCs stably transfected with the A allele of rs3716, the differentiation of mNSCs stably expressing the rs3617 C allele into neurons (MAP2positive) was significantly increased. **E** and **F**: Representative immunostaining images (**E**) and corresponding quantification (**F**) of immature postmitotic neurons which are TUJ1 positive. Data are represented as mean ± SD, and *P* values were calculated using two-tailed Student's *t*-test, $n = 3$ and a total of 11 immunostaining images were used for cell counting for **B**; $n = 3$ and a total of 15 immunostaining images were used for cell counting for **D**; $n = 3$ and a total of 15 immunostaining images were used for cell counting for **F**. Scale bar represents 50 μm in **A**, **C**, and **E**. **, $P < 0.01$, ***, $P < 0.001$. mNSC, mouse neural stem cell; SD, standard deviation.

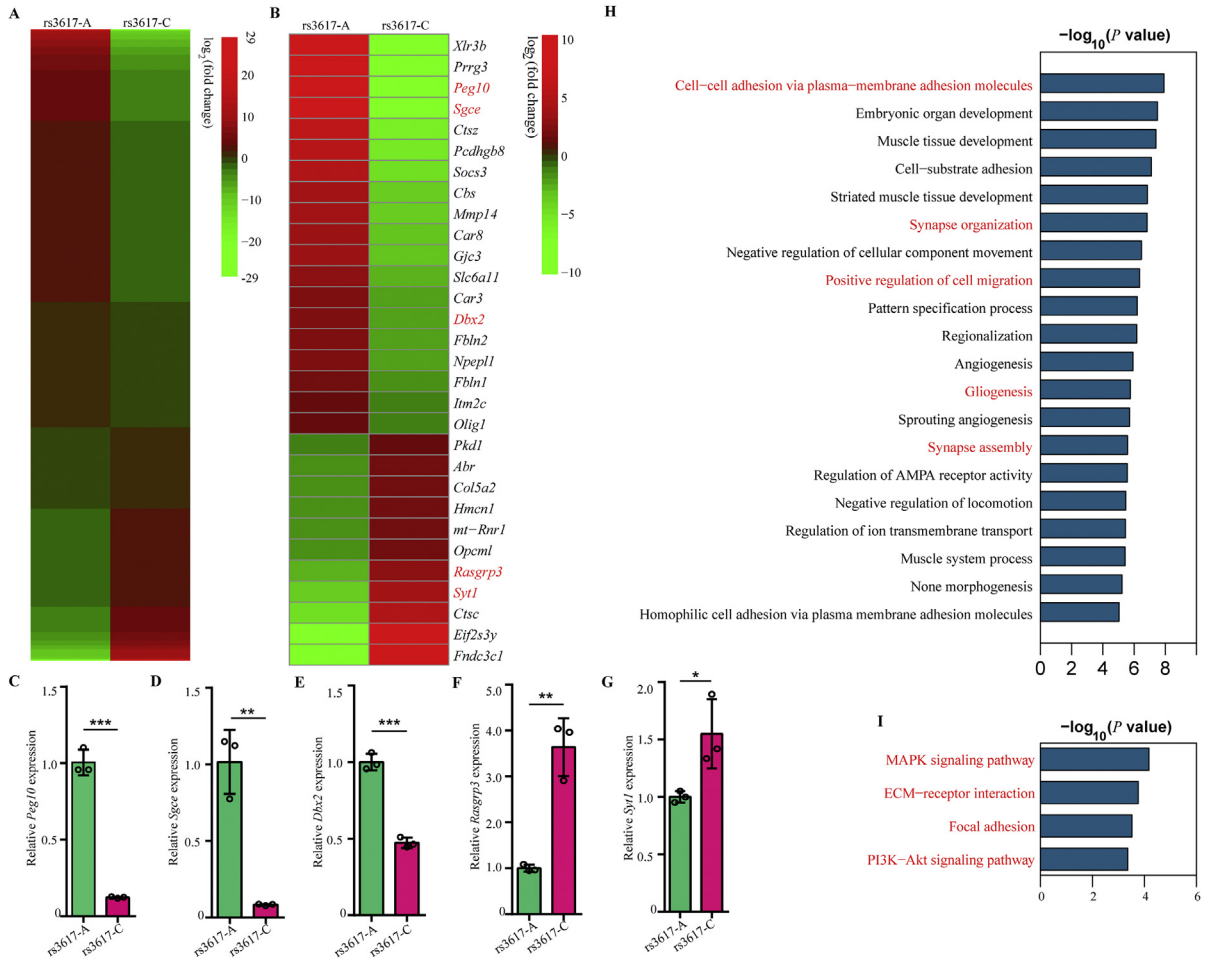

Fig. 6. Transcriptome analysis revealed differentially expressed genes between mNSCs stably transfected with the C and A allele of rs3617. **A**: Expression heat map showing the differentially expressed genes ($n = 669$) between mNSCs stably transfected with the C and A allele of rs3617. **B**: The top 30 genes showing the most significant expression differences. **C–G**: Quantitative PCR (qPCR) validation of RNA-Seq results. Genes marked with red color in **B** were selected for qPCR verification. These genes included *Peg10* (**C**), *Sgce* (**D**), *Dbx2* (**E**), *Rasgrp3* (**F**) and *Syt1* (**G**). Data are represented as mean ± SD, and *P* values were calculated using two-tailed Student's *t*-test. Average results of three independent biological replicates are presented (three technical replicates for each biological replicate). *, $P < 0.05$; **, $P < 0.01$; ***, $P < 0.001$. **H**: Gene Ontology (GO) analysis for differentially expressed genes identified by RNA-Seq. The differentially expressed genes were significantly enriched in neurodevelopment-related pathways, including cell adhesion, synapse organization, cell migration, and gliogenesis. **I**: KEGG analysis for differentially expressed genes identified by RNA-Seq. The differentially expressed genes were significantly enriched in MAPK, ECM-receptor interaction, adhesion, and PI3K-AKT signaling pathways. mNSC, mouse neural stem cell; RNA-Seq, RNA sequencing; KEGG, Kyoto Encyclopedia of Genes and Genomes; SD, standard deviation.

2010; Franco and Muller, 2011). Considering the important roles of the extracellular matrix in brain development and function, it is possible that *ITIH3* may confer SZ risk by affecting the function of the extracellular matrix, which in turn influences neurodevelopment. Consistent with this, we found that mNSCs stably overexpressing different alleles of rs3617 exhibited significant differences in proliferation, migration, and differentiation. Our comparative analysis of the transcriptomes in mNSCs stably overexpressing different alleles at rs3617 also supports the hypothesis that rs3617 may participate in SZ pathogenesis by affecting neurodevelopment. Intriguingly, this contention is further strengthened by the observation that differentially expressed genes in cells carrying different alleles at rs3617 were significantly enriched in neurodevelopment-related pathways, including cell adhesion, cell migration, gliogenesis, and synapse organization. In addition, KEGG analysis highlighted enrichment of these differentially expressed genes in MAPK and PI3K-AKT signaling pathways, two pathways with pivotal roles in SZ (Emamian et al., 2004; Funk et al., 2012).

Of note, we found that the human ITIH3 protein harboring the rs3617 C allele (risk allele) increased the proliferation of mNSCs and promoted the differentiation of mNSCs into $MAP2^+$ and $TUJ1^+$ neuronal cells. Although previous studies have shown that down-regulation of several SZ risk genes (including *DISC1* and *RELN*) inhibited proliferation of NSCs (Won et al., 2006; Mao et al., 2009; Ishizuka et al., 2011), several studies also showed that down-regulation of SZ risk genes (*GLT8D1* and *VRK2*) could increase proliferation of NSCs (Yu et al., 2017; Yang et al., 2018). In the present study, the SZ risk C allele of rs3617 is associated with lower ITIH3 protein expression, and it is possible that human ITIH3 protein harboring the C allele at rs3617 increased the proliferation of mNSCs through mechanisms similar to *GLT8D1* and *VRK2*. In addition, we noticed that migration of mNSCs carrying the rs3617 C allele was significantly impaired compared with those carrying the rs3617 A allele (Fig. 4). Therefore, the human ITIH3 protein corresponding to the SZ risk C allele of rs3617 likely affects both proliferation and migration processes that are essential for proper neurodevelopment. Finally, we found that differentiation of mNSCs into glial cells was significantly impaired when the cells stably overexpressed ITIH3 and rs3617 C allele (Fig. 5A and B), suggesting that rs3617 may affect the appropriate ratios of neuronal and glial

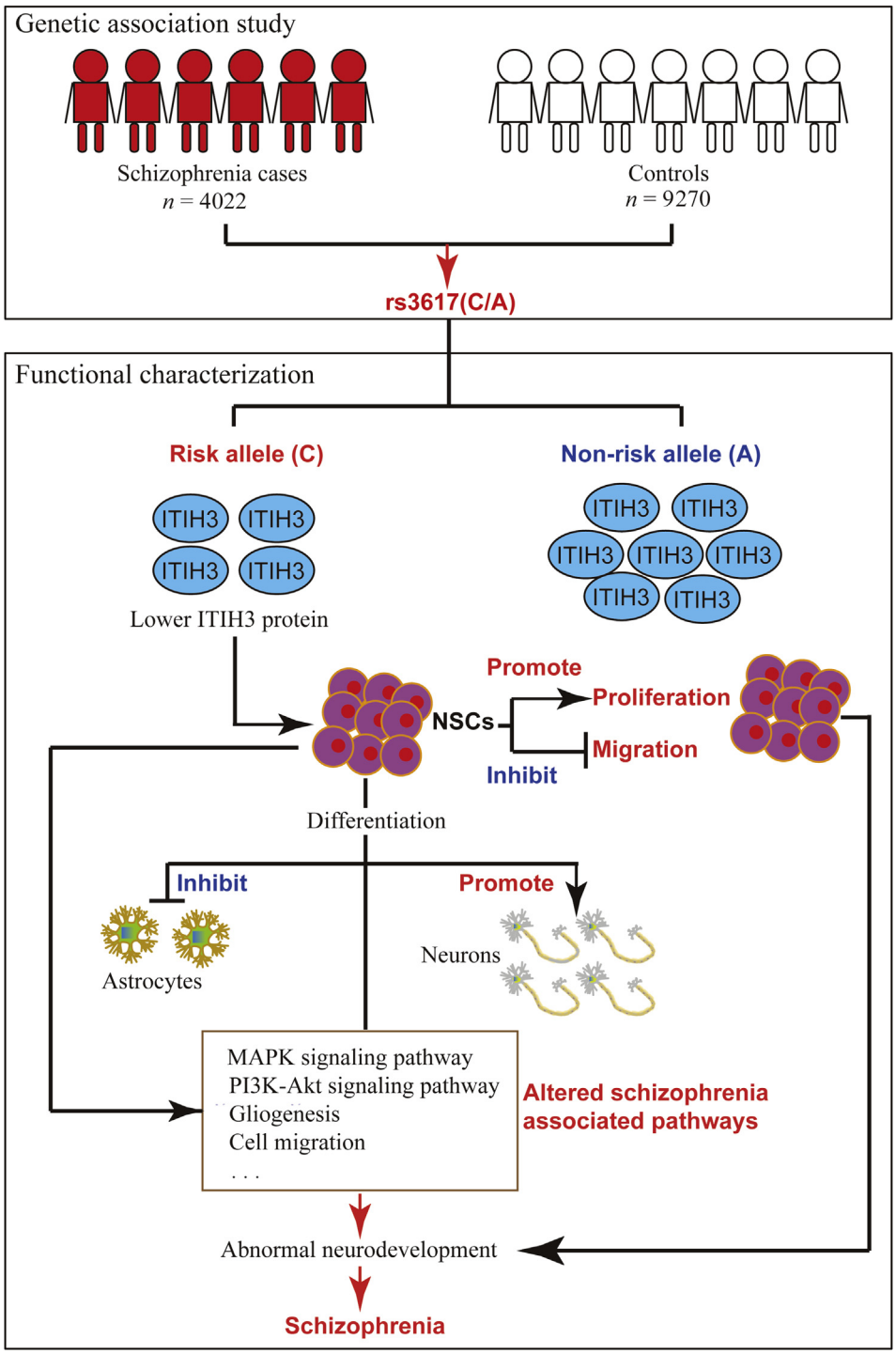

Fig. 7. The working model of rs3617 in schizophrenia pathogenesis. The schizophrenia risk C allele of rs3617 downregulates ITIH3 expression. Lower ITIH3 expression promotes proliferation of NSCs but inhibits their migration. Lower ITIH3 expression promotes differentiation of NSCs into glial cells but inhibits their differentiation into neurons. Single Nucleotide Polymorphism (SNP) rs3617 also alters schizophrenia-associated pathways. These results together suggest that rs3617 may confer risk of schizophrenia by affecting neurodevelopment. NSC, neural stem cell.

cells in the brain. Taken together, these data strongly suggest that rs3617 affects neurodevelopment by regulating proliferation, migration, and differentiation of NSCs and thereby contributes to SZ pathogenesis.

In both GTEx and LIBD brain eQTL data sets, no significant association between rs3617 and *ITIH3* mRNA expression was observed. A possible explanation is that rs3617 may exert greater effect on the protein levels of ITIH3 but less impact on mRNA expression. We compared the effect size of different alleles of rs3617 on mRNA and protein levels of ITIH3 in triplicated samples. In HEK293 cells, we found that the effect of rs3617 on *ITIH3* mRNA expression was more significant than that on ITIH3 protein. Compared with cells transfected with the A allele of rs3617, cells transfected with the C allele exhibited a 42% reduction of *ITIH3*

mRNA, but only 20% reduction of the protein. However, in mNSCs, we found that the effect of rs3617 on ITIH3 protein expression was more significant than that on the *ITIH3* mRNA expression level. Specifically, the *ITIH3* mRNA level was reduced by 25%, and the ITIH3 protein level was reduced by 31% in NSCs transfected with the C allele of rs3617 compared with those transfected with the A allele. However, it is also possible that rs3617 may exert its main effects by regulating expression of other genes (or affecting ITIH3 activity). More work is needed to examine the potential impact of rs3617 on other genes.

Despite the enlightening discoveries, there are several limitations to this study. First, eight coding SNPs were successfully genotyped in our study; however, only rs3617 showed a genome-wide significant association with SZ. Nevertheless, we noticed that 5 of the other 7 (including rs950169, rs4584886, rs2288920, rs20551, and rs133335) coding SNPs have the same allelic direction of their effects in both the PGC and our sample. Considering that the PGC sample size is much larger than that of the present study, these SNPs may show significant associations with SZ in the Chinese population as the sample size increases. In addition, considering the genetic heterogeneity (i.e., different genetic variants in a gene were associated with SZ in different populations) of SZ (Li et al., 2011; Yue et al., 2011), it is also possible that other genetic variants, which were not highlighted in PGC, confer causative risk of SZ in Chinese individuals. More work is thus needed to investigate the association between SZ and other SNPs of these loci in the Han Chinese population. Second, we have shown that rs3617 is a functional nonsynonymous SNP. However, we still do not know how different amino acids encoded by rs3617 affect the function of ITIH3 protein. It is possible that p.K315Q may influence the biological function of ITIH3 rather than its localization. More work is needed to investigate the precise mechanisms. Third, we investigated the potential functional consequences and biological effects of rs3617 by overexpressing the ITIH3 proteins containing different amino acids at rs3617. Although our results suggest that endogenous *ITIH3* expression may not affect our results significantly, potential bias might still be introduced as the use of overexpression vectors leads to much higher levels of ITIH3 protein in these cells than the physiological level. Ideally, additional analyses using genomic editing techniques (e.g., CRISPR-Cas9–mediated single-base editing) to obtain cells having different alleles of rs3617 while expressing ITIH3 at the physiological level are needed. Fourth, most of the results of this study were from *in vitro* assays, and *in vivo* validation of the functional consequences of rs3617 using mice carrying different alleles of rs3617 is needed. For example, CRISPR-Cas9–mediated single-base editing might allow the generation of these mice. Physiological and pathological evaluation of these mice will then provide pivotal information about the role of rs3617 in SZ pathogenesis. Finally, in differentiation assays, although mNSCs underwent differentiation for 4.5 days in the differentiation medium, it might still be possible that a very small proportion of progenitor cells (GFAP-positive) remained in the final cell populations, which affected the ratio of GFAP-positive cells we calculated. Further validation is needed to differentiate these GFAP-positive progenitors and glial cells in the final cell populations.

In summary, we have shown that rs3617 is significantly associated with SZ in the Han Chinese population (with the same risk allele as in the European population), indicating that rs3617 is a common risk variant for SZ across different ethnicities. We have also confirmed that rs3617 is a functional missense SNP, which exerts biological effect on SZ by affecting neurodevelopment. Finally, we have identified genes differentially expressed in mNSCs stably transfected with different alleles of rs3617 and have found significant enrichment of these genes in multiple signaling pathways essential for physiological homeostasis and neurodevelopment (e.g., MAPK and PI3K-AKT signaling pathways), suggesting that rs3617 may confer risk of SZ by modulating these pathways. Our study demonstrates how a coding SNP (rs3617) confers risk of SZ by affecting ITIH3 function, shedding new light on the genetic mechanisms of SZ.

4. Materials and methods

4.1. Study participants

A total of 4022 unrelated SZ cases and 9270 controls were included in this study. Detailed information about the cases and controls has been described in our previous studies (Luo et al., 2008; Li et al., 2011; Ma et al., 2013; Zhang et al., 2014). In brief, the samples included in this study were mainly recruited from Hunan (Ma et al., 2013; Zhang et al., 2014) (Institute of Mental Health, National Clinical Research Center for Mental Health Disorders and National Technology Institute of Psychiatry, The Second Xiangya Hospital, Central South University) and Yunnan (Luo et al., 2008; Li et al., 2011) (Yunnan Mental Health Center) provinces (two geographically dispersed regions of China) of China. To guarantee the quality of each participant included in this study, the detailed information (including the onset and course of psychosis, symptoms, family history of psychiatric illnesses, personal and family history report, and medical reports were collected) of each case was collected and carefully assessed by experienced psychiatrists. All the unrelated participants were of Han Chinese origin, and the cases were diagnosed with SZ according to DSM-IV or ICD-10 criteria. Diagnoses were performed by experienced psychiatrists, and individuals with a history of neurological diseases, drug abuse, and alcohol abuse were excluded in this study. The ages of the cases and controls were 28 ± 13.28 and 38 ± 12.06 years, respectively. Written informed consent was obtained from all participants, and this study was approved by the Internal Review Board of Kunming Institute of Zoology, Chinese Academy of Sciences.

4.2. Genomic DNA extraction and genotyping

We used the standard phenol-chloroform method to extract genomic DNA (from peripheral blood). The eight potential causal coding SNPs are shown in Table 1. Although 10 potential causal coding SNPs were identified by the PGC (Schizophrenia Working Group of the Psychiatric Genomics Consortium, 2014), only eight nonsynonymous exonic SNPs were included in this study as rs13107325 is monomorphic in the Chinese population according to the 1000 Genomes project (Abecasis et al., 2010) and rs2955365 failed to be genotyped. Genotyping was performed using the SNaPshot approach, which uses a single-base extension principle to genotype the desired SNPs. Detailed procedures for DNA extraction and genotyping can be found in our previous study (Luo et al., 2008). In brief, we first amplified the genomic sequence containing the tested SNP by PCR (the PCR primers are provided in Table S6). We then treated the PCR products with shrimp alkaline phosphatase (Takara, Osaka, Japan) and exonuclease I (Takara) to remove the unincorporated dNTPs and primers. PCR was conducted again using the purified products, SNaPshot multiplex mix, genotyping primers (the genotyping PCR primers are provided in Table S7), and ddNTPs. The 3′ end of the genotyping primer stops just one base before the test SNP, so the polymerase extends the primer by one nucleotide (adding a single ddNTP to its 3′ end). As the ddNTPs were labeled with different fluorescence colors, the fluorescence color readout reports which base was added. Electrophoresis was performed using the 3730 DNA analyzer (Applied Biosystems, Foster, USA), and the data were analyzed using

GeneMapper software (Applied Biosystems). Genotypes of each SNP were manually checked. The genotyping results were validated with Sanger sequencing by sequencing 100 randomly selected individuals, and no genotyping errors were observed.

4.3. Genetic association analysis

The HWE for each SNP was assessed using PLINK (Boston, USA) (Purcell et al., 2007). The allelic association test of each SNP was conducted using the chi-square test (implemented in PLINK) (Purcell et al., 2007). Meta-analysis was performed as previously described (Li et al., 2018), and the fixed-effect model was used.

4.4. Sequence conservation and 3D structure analyses

The protein sequences of 35 vertebrate species surrounding p.K315Q (rs3617) were extracted from the UCSC Genome Browser (https://genome.ucsc.edu/). The 3D structures of ITIH3 containing lysine and glutamine amino acids at rs3617 were simulated with SWISS-MODEL (https://swissmodel.expasy.org/).

4.5. LD analysis

We examined the LD patterns of the genomic regions containing the eight tested nonsynonymous SNPs using the genotype data (phase 3) from the 1000 Genomes project (The 1000 Genomes Project Consortium, 2015). In brief, genotype data (±5 kb of the nonsynonymous SNP) of 99 Europeans (CEU) and 103 Chinese (CHB) participants were downloaded. LD maps were generated using Haploview (Cambridge, USA) (Barrett, 2009), and LD values were presented as r^2. We performed SNP filtering before plotting the LD plot. Our SNP filtering parameters are as follows: Hardy-Weinberg *P*-value ≥0.01, genotyping rate ≥75%, and minor allele frequency ≥0.01. We used the default algorithm (based on confidence interval, which was developed by Gabriel et al. (2002)) implemented in Haploview software (Barrett et al., 2005; Barrett, 2009) to define LD blocks. This algorithm first labels comparison between variants as "strong LD," "inconclusive," and "strong recombination" based on 95% confidence bounds on D prime (D ') for each comparison. Then, a block is defined if 95% of informative comparisons are labeled as "strong LD." More detailed information about the definition of LD blocks can be found in previous articles (Gabriel et al., 2002; Barrett et al., 2005). To make sure that the generated LD plot is centered on the exonic variant, we first extracted the SNP surrounding the exonic variant (±10 kb). We then selected SNPs manually to guarantee that each exonic SNP has the same (or similar) number of upstream and downstream variants.

4.6. eQTL analysis

To explore if rs3617 was associated with gene expression in human brain tissues, we examined the associations between rs3617 and gene expression using the brain eQTL data from GTEx (The GTEx Consortium, 2015) and LIBD (eQTL of dorsolateral prefrontal cortex tissues from 412 participants) (Jaffe et al., 2018) data sets. Detailed information about the GTEx and LIBD brain eQTL data can be found in the original publications (The GTEx Consortium, 2015; Jaffe et al., 2018).

4.7. Construction of ITIH3 expression vector and transfection

To explore the impact of different alleles of rs3617 on ITIH3 protein expression, we constructed ITIH3 expression constructs by cloning the full-length coding sequence of human *ITIH3* (2670 bp) into the pEGFP-N2 vector. Two expression vectors carrying different alleles (either the C or A allele) at rs3617 and the same sequence otherwise were constructed. The sequence of *ITIH3* was inserted into *Xho*I and *Kpn*I restriction sites of pEGFP-N2, and the inserted sequence of *ITIH3* was validated by direct sequencing. To quantify ITIH3 expression, Green Fluorescent Protein (GFP) was fused to the C-terminus of ITIH3. Equal amounts of *ITIH3* expression vectors (containing either the C or A allele of rs3617) were transfected into HEK293 cells using the polyethylenimine (PEI) (Polyscience, Warrington, USA) reagent.

4.8. Isolation and characterization of mNSCs

mNSCs were isolated as previously described (Azari et al., 2011; Yang et al., 2018). In brief, brains of mouse embryos (E13.5) were harvested, and ganglionic eminences were dissected. The dissected brains were microdissected, and brain tissues were dissociated thoroughly through repeated pipetting. The cell suspension was then transferred to a new tube and centrifuged at 110 *g* for 5 min at room temperature. The supernatant was discarded, and the cells were resuspended to make a homogeneous single-cell suspension. The cells were then plated at the density of ~3×10^5 cells/mL in NSC medium (STEMCELL, Vancouver, Canada). The mNSCs were cultured in NeuroCult™ Basal Medium (STEMCELL), which was supplemented with 10% proliferation supplement (STEMCELL, NeuroCult™ Proliferation Supplement [mouse and rat]), 20 ng/mL of epidermal growth factor (STEMCELL), 20 ng/mL of basic fibroblast growth factor (STEMCELL), and 2 μg/mL of heparin (STEMCELL). After culturing for 3–5 days, neurospheres formed by mNSCs were used for further experiments and passaging. We used three well-characterized NSC markers (SOX2, PAX6, and NESTIN) to characterize the isolated mNSCs.

4.9. Construction of NSCs stably overexpressing ITIH3

To investigate if the different alleles of rs3617 have different effects on proliferation, differentiation, and migration of mNSCs, we generated mNSCs that overexpress *ITIH3* stably. In brief, the full-length coding sequence of human *ITIH3* (2673 bp, containing TGA terminator) was cloned into the pCDH lentiviral vector at multiple clone sites *Eco*RI and *Not*I. Flag tag (3 ×) was fused to the N-terminus of *ITIH3*. To produce functional lentiviral particles, the cloned pCDH vectors (containing either the A or C allele of rs3617), psPAX2 and pMD2G vectors (obtained from the laboartory of Prof. Yongbin Chen), were co-transfected into HEK293T cells using PEI. Cell culture supernatants were collected at 48 h and 72 h after transfection, respectively. The supernatants were then concentrated and used to infect mNSCs. Twenty-four hours after infection, mNSCs were treated with puromycin (2 μg/mL) for 14 days to select cells that were stably transfected with *ITIH3* overexpression vectors.

4.10. Cell culture

The HEK293 and HEK293T cells, originally from the American Type Culture Collection, were obtained from Shanghai Cell Bank (Shanghai, China), Chinese Academy of Sciences. The cells were cultured in Dulbecco's modified Eagle's medium (DMEM, Thermo, Waltham, USA) supplemented with 10% fetal bovine serum (Gibco, New York, USA) and penicillin/streptomycin (100 U/mL of penicillin and 0.1 mg/mL of streptomycin; HyClone, Logan, USA) at 37 °C in 5% CO_2. Periodic testing was conducted to ensure that no mycoplasma contamination occurred in these cell lines during the present study.

4.11. BrdU proliferation assays

To compare the effect of different alleles of rs3617 on proliferation, we performed BrdU (a nucleoside analog) incorporation assays. The HEK293 cells were plated in 24-well plates at a density of 4×10^4 per well. After 24 h, equal amount of *ITIH3* overexpression vectors with either the C allele or A allele of rs3617 was transfected into the HEK293 cells. When the cell density reached ~80%–90% confluence (48 h after transfection), 10 μM BrdU (Sigma, St. Louis, USA) was added to each well and incubated for 1 h. The cells were then fixed with 4% Paraformaldehyde (PFA) and permeabilized with 0.3% Triton X-100 (Promega, Madison, USA). After three washes with phosphate-buffered saline (PBS), 2 M HCl was added to denature DNA at 37 °C for 30 min. The cells were then blocked with blocking buffer at room temperature for 1 h, followed by incubation with the primary antibody (rat anti-BrdU, 1:1000, cat# NB500-169; Novas, Littleton, USA) overnight at 4 °C and secondary antibody (1:500, cat# A10522; Life Technologies, New York, USA) for 1 h at room temperature. We also carried out BrdU incorporation assays for mNSCs stably overexpressing *ITIH3*. Immunofluorescence staining images were obtained using a confocal microscope (FV1000; Olympus, Tokyo, Japan). The number of cells was counted using ImageJ software (National Institutes of Health, Bethesda, USA) (https://imagej.nih.gov/ij/). A total of 10 immunostaining images from three biological replicates were used for cell counting.

4.12. CCK-8 assays

The HEK293 cells were seeded into 96-well plates (3×10^3 per well). After 24 h, the cells were transfected with the following expression vectors: pEGFP, pEGFP-*ITIH3*-C allele, and pEGFP-*ITIH3*-A allele. These vectors express GFP, ITIH3 protein with glutamine (p.315Q) at rs3617, ITIH3 protein with lysine (p.315K) at rs3617, respectively. Forty-eight hours after transfection, CCK-8 (Beyotime, China) was used to measure the proliferation rate of cells following the manufacturer's instruction. A spectrophotometer was used to measure the absorbance of each well at wavelengths of 450 nm and 630 nm. Cell viability was quantified by subtracting the background absorbance at 630 nm from the absorbance at 450 nm. We also tested the impact of different alleles of rs3617 on the proliferation of mNSCs using the same method. Five biological replicates were used for each experimental condition.

4.13. Differentiation of NSCs into neurons and glia cells

The mNSCs stably overexpressing *ITIH3* and carrying either the C or A allele at rs3617 were seeded (1×10^5 cells/well) into 24-well plates precoated with 10 μg/mL of laminin. To differentiate the mNSCs into neuronal and glial cells, we used the following differentiation medium: DMEM/F12 (Gibco), B27 (Gibco), N-2 (Gibco), and heparin (STEMCELL Technologies). After differentiation for 4.5 days, immunostaining was performed to count the number of neuronal and glial cells. In brief, the cells were fixed with 4% PFA, permeabilized with PBS containing 0.3% Triton-X100, and then blocked with blocking buffer (Beyotime) for 1 h at room temperature. The cells were then incubated with primary antibodies overnight at 4 °C, followed by incubation with species-specific fluorescent secondary antibodies at room temperature for 1 h. The primary antibody used in differentiation assays were as follows: GFAP (1:2000, cat# G9269; Sigma), TUJ1 (1:500, cat# ab78078; Abcam, Cambridge, England), and MAP2 (1:500, cat# AB5622; Millipore, Massachusetts, USA). The secondary antibodies were as follows: Alexa Fluor 488 donkey anti-rabbit (1:500; Life Technologies) and Alexa Fluor 568 donkey anti-mouse (1:500; Life Technologies). A total of 11 immunostaining images from three biological replicates were used to count GFAP-positive cells. A total of 15 immunostaining images from three biological replicates were used to count MAP2- and TUJ1-positive cells.

4.14. Migration assays of NSCs

Migration assay was performed as previously described (Kong et al., 2008; Li et al., 2017). In brief, neurospheres with similar diameters were selected and plated in 24-well plates (precoated with laminin). Only one neurosphere was seeded into each well. After culturing neurospheres in NeuroCult™ Basal Medium (STEMCELL) supplemented with 10% differentiation supplement (STEMCELL, NeuroCult™ Differentiation Supplement [mouse]) for 24 h, the migration distance of neurospheres was quantified by subtracting the radius of the original neurosphere from the radius of the neurosphere at 24 h using ImageJ software. Migration distance of five neurospheres was analyzed for each group (i.e., NSCs stably transfected with the control vector pCDH, *ITIH3*-expressing vectors containing the C allele at rs3617, and *ITIH3*-expressing vector containing the A allele at rs3617).

4.15. Western blotting

Total proteins were extracted using the RIPA buffer (Thermo, Waltham, USA) containing 1% Phenylmethanesulfonyl fluoride (PMSF) (Beyotime, Shanghai, China). Protein concentration was quantified using the bicinchoninic acid protein assay kit (Thermo). After subjecting to 10% Sodium Dodecyl Sulfate (SDS)-polyacrylamide gel electrophoresis, the proteins were transferred to a polyvinylidene difluoride (PVDF) membrane. Five percent of defatted milk was used to block nonspecific binding. The PVDF membrane was then incubated with primary antibodies overnight at 4 °C, followed by three washes with Tris-Hcl Buffer Solution added Tween (TBST) and then incubated with secondary antibodies for 1 h at room temperature. The SuperSignal West Pico Chemiluminescent Substrate (Thermo) was used for protein detection. The primary antibodies used in the Western blotting assay included: mouse anti-GFP (1:100, cat# sc-9996; Santa Cruz, Santa Cruz, USA), rabbit anti-ACTB (1:1000, cat# D110001-0200; Sangon, Shanghai, China), rabbit anti-FLAG (1:1000, cat# F7425; Sigma). The secondary antibodies were as follows: Horseradish Peroxidase (HRP)-labeled goat anti-mouse IgG (H + L) (1:1000, cat# A0216; Beyotime) and HRP-labeled goat anti-rabbit IgG (H + L) (1:1000, cat# A0208; Beyotime).

4.16. Protein degradation assays (CHX chase analysis)

To test if lysine and glutamine corresponding to different alleles of rs3617 at the 315th amino acid of ITIH3 affected its stability, we conducted CHX chase analysis. CHX is a translation inhibitor that inhibits eukaryotic translation and protein synthesis. As protein translation is inhibited by CHX, no new proteins can be synthesized after CHX treatment. The CHX chase assay is therefore widely used to analyze protein degradation (Buchanan et al., 2016). In brief, 1.5×10^5 HEK293T cells were plated into each well of 12-well plates. The day after cell plating, the cells were transfected with either *ITIH3*-rs3617-A or *ITIH3*-rs3617-C expression plasmids. Glutathione S-transferase plasmids were co-transfected to control for transfection efficiency. Twenty-four hours after transfection, the cells were treated with 50 μg/mL of CHX at indicated time points and harvested for Western blotting analysis.

4.17. Real-time quantitative PCR

Total RNA was extracted using Trizol Reagent (Life Technologies). After removing potential genomic DNA contamination using the PrimeScript™ RT reagent Kit with gDNA Eraser (Perfect Real Time) (Takara, Osaka, Japan), reverse transcription was performed using the Takara Reverse Transcription System (PrimeScript™ RT reagent Kit). RT-qPCR was performed using the TB Green Premix Ex Taq II kit (Takara). Beta-actin (*ACTB*) was used as the internal control. Gene expression levels were analyzed and presented using the $2^{-\Delta\Delta Ct}$ method (Livak and Schmittgen, 2001). The real-time qPCR primers are provided in Table S8.

4.18. Transcriptome analysis by RNA-Seq

Total RNA of mNSCs stably overexpressing *ITIH3* (containing either the C or A allele at rs3617) was extracted using the Trizol reagent (Invitrogen, Carlsbad, USA). RNA concentration was quantified using Qubit®3.0 Fluorometer (Life Technologies). RNA purity was determined using the NanoPhotometer® spectrophotometer (IMPLEN, CA, USA), and RNA integrity was assessed using the Bioanalyzer 2100 system (Agilent Technologies, CA, USA). Three micrograms of total RNA from each sample was used to construct sequencing libraries according to the recommendations of the NEBNext® Ultra™ RNA Library Prep Kit for Illumina® (#E7530L, NEB, Ipswich, USA), and different index codes were used to generate sequencing libraries. After initial quantification, oligo (dT) and fragmentation buffer were used to enrich and then fragment mRNA. The fragmented mRNA was then reverse transcribed into cDNA using random primers. The purified double-strand cDNA was then end repaired, tailed, and ligated. Paired-end RNA-Seq (Illumina, San Diego, USA) was performed to quantify gene expression levels.

Clean reads were mapped to the mouse genome (GRCm38) using hisat2 (Kim et al., 2015) (version 2.1.0) with default parameters. Stringtie (Pertea et al., 2015) (version 1.3.4) was used to assemble transcripts with default parameters. DEseq2 (Love et al., 2014) (implemented in R [version 3.5.1]) was used to identify differentially expressed genes. Bonferroni correction was conducted to correct *P* values. Genes with $|\log2FC| \geq 1$ and adjusted *P* value (Padj) ≤ 0.05 were defined as significantly differentially expressed genes. GO and KEGG enrichment analyses were performed using ClusterProfiler (Yu et al., 2012) in R (version 3.5.1, https://www.r-project.org/).

4.19. Dosage effect assay

Equal amounts of HEK293 cells (1×10^5) were plated into 96-well plates and cultured for 18 h. Then, the cells were transfected with different amounts of ITIH3-overexpressing vectors (0.5, 1.0, 1.5, and 2.0 μg, respectively). Forty-eight hours after transfection, cell viability was determined using the CCK-8 assays.

4.20. Statistical analysis

The associations between the genotyped SNPs and SZ were analyzed using PLINK (chi-square test) (Purcell et al., 2007). Meta-analysis was performed as previously described (Li et al., 2018), and the fixed-effect model was used. For ITIH3 protein quantification experiments, assays for analysis of proliferation, migration, and differentiation of NSCs, and qPCR experiments, two-tailed Student's *t*-test was used, and significance threshold was set at $P < 0.05$.

CRediT authorship contribution statement

Kaiqin Li: Data curation, Formal analysis, Investigation, Methodology, Validation, Visualization, Writing - original draft. **Yifan Li:** Data curation, Formal analysis, Investigation, Methodology, Validation, Visualization, Writing - original draft. **Junyang Wang:** Data curation, Formal analysis, Investigation, Methodology, Validation, Visualization, Writing - original draft. **Yongxia Huo:** Data curation, Formal analysis, Investigation, Methodology, Validation, Visualization, Writing - original draft. **Di Huang:** Data curation, Formal analysis, Investigation, Methodology, Validation, Visualization, Writing - original draft. **Shiwu Li:** Data curation, Formal analysis, Investigation, Methodology, Validation, Visualization, Writing - original draft. **Jiewei Liu:** Data curation, Formal analysis, Investigation, Methodology, Validation, Visualization, Writing - original draft. **Xiaoyan Li:** Data curation, Formal analysis, Investigation, Methodology, Validation, Visualization, Writing - original draft. **Rong Liu:** Data curation, Formal analysis, Investigation, Methodology, Validation, Visualization, Writing - original draft. **Xiaogang Chen:** Conceptualization, Project administration, Resources, Supervision, Writing - review & editing. **Yong-Gang Yao:** Conceptualization, Project administration, Resources, Supervision, Writing - review & editing. **Ceshi Chen:** Conceptualization, Project administration, Resources, Supervision, Writing - review & editing. **Xiao Xiao:** Conceptualization, Project administration, Resources, Supervision, Writing - review & editing. **Ming Li:** Conceptualization, Project administration, Resources, Supervision, Writing - review & editing. **Xiong-Jian Luo:** Conceptualization, Project administration, Resources, Supervision, Writing - review & editing.

Acknowledgments

This study was equally supported by the National Natural Science Foundation of China of China (31970561 and 31722029 to X.-J.L.), the National Key Research and Development Program of China (Stem Cell and Translational Research) (2016YFA0100900), the Innovative Research Team of Science and Technology department of Yunnan Province (2019HC004), and the Key Research Project of Yunnan Province (2017FA008 to X.-J.L.).

Supplementary data

Supplementary data to this article can be found online at https://doi.org/10.1016/j.jgg.2020.04.001.

References

Abecasis, G.R., Altshuler, D., Auton, A., Brooks, L.D., Durbin, R.M., Gibbs, R.A., Hurles, M.E., McVean, G.A., 2010. A map of human genome variation from population-scale sequencing. Nature 467, 1061–1073.

Allen, N.C., Bagade, S., McQueen, M.B., Ioannidis, J.P., Kavvoura, F.K., Khoury, M.J., Tanzi, R.E., Bertram, L., 2008. Systematic meta-analyses and field synopsis of genetic association studies in schizophrenia: the SzGene database. Nat. Genet. 40, 827–834.

Azari, H., Sharififar, S., Rahman, M., Ansari, S., Reynolds, B.A., 2011. Establishing embryonic mouse neural stem cell culture using the neurosphere assay. J. Vis. Exp. 47, 2457.

Barrett, J.C., 2009. Haploview: visualization and analysis of SNP genotype data. Cold Spring Harb. Protoc. 2009, pdb.ip71.

Barrett, J.C., Fry, B., Maller, J., Daly, M.J., 2005. Haploview: analysis and visualization of LD and haplotype maps. Bioinformatics 21, 263–265.

Barros, C.S., Franco, S.J., Muller, U., 2010. Extracellular matrix: functions in the nervous system. Cold Spring Harb. Perspect. Biol. 3, a005108.

Bost, F., Diarra-Mehrpour, M., Martin, J.P., 1998. Inter-alpha-trypsin inhibitor proteoglycan family–a group of proteins binding and stabilizing the extracellular matrix. Eur. J. Biochem. 252, 339–346.

Buchanan, B.W., Lloyd, M.E., Engle, S.M., Rubenstein, E.M., 2016. Cycloheximide chase analysis of protein degradation in *Saccharomyces cerevisiae*. J. Vis. Exp. 110, 53975.

Buckley, P.F., Miller, B.J., Lehrer, D.S., Castle, D.J., 2009. Psychiatric comorbidities and schizophrenia. Schizophr. Bull. 35, 383–402.

Chen, C., Meng, Q., Xia, Y., Ding, C., Wang, L., Dai, R., Cheng, L., Gunaratne, P., Gibbs, R.A., Min, S., Coarfa, C., Reid, J.G., Zhang, C., Jiao, C., Jiang, Y., Giase, G., Thomas, A., Fitzgerald, D., Brunetti, T., Shieh, A., Xia, C., Wang, Y., Badner, J.A., Gershon, E.S., White, K.P., Liu, C., 2018. The transcription factor POU3F2 regulates a gene coexpression network in brain tissue from patients with psychiatric disorders. Sci. Transl. Med. 10, eaat8178.

Colombatti, A., Bonaldo, P., 1991. The superfamily of proteins with von Willebrand factor type A-like domains: one theme common to components of extracellular matrix, hemostasis, cellular adhesion, and defense mechanisms. Blood 77, 2305–2315.

Diarra-Mehrpour, M., Sarafan, N., Bourguignon, J., Bonnet, F., Bost, F., Martin, J.P., 1998. Human inter-alpha-trypsin inhibitor heavy chain H3 gene. Genomic organization, promoter analysis, and gene linkage. J. Biol. Chem. 273, 26809–26819.

Emamian, E.S., Hall, D., Birnbaum, M.J., Karayiorgou, M., Gogos, J.A., 2004. Convergent evidence for impaired AKT1-GSK3beta signaling in schizophrenia. Nat. Genet. 36, 131–137.

Franco, S.J., Muller, U., 2011. Extracellular matrix functions during neuronal migration and lamination in the mammalian central nervous system. Dev. Neurobiol. 71, 889–900.

Fromer, M., Pocklington, A.J., Kavanagh, D.H., Williams, H.J., Dwyer, S., Gormley, P., Georgieva, L., Rees, E., Palta, P., Ruderfer, D.M., Carrera, N., Humphreys, I., Johnson, J.S., Roussos, P., Barker, D.D., Banks, E., Milanova, V., Grant, S.G., Hannon, E., Rose, S.A., Chambert, K., Mahajan, M., Scolnick, E.M., Moran, J.L., Kirov, G., Palotie, A., McCarroll, S.A., Holmans, P., Sklar, P., Owen, M.J., Purcell, S.M., O'Donovan, M.C., 2014. *De novo* mutations in schizophrenia implicate synaptic networks. Nature 506, 179–184.

Funk, A.J., McCullumsmith, R.E., Haroutunian, V., Meador-Woodruff, J.H., 2012. Abnormal activity of the MAPK- and cAMP-associated signaling pathways in frontal cortical areas in postmortem brain in schizophrenia. Neuropsychopharmacology 37, 896–905.

Gabriel, S.B., Schaffner, S.F., Nguyen, H., Moore, J.M., Roy, J., Blumenstiel, B., Higgins, J., DeFelice, M., Lochner, A., Faggart, M., Liu-Cordero, S.N., Rotimi, C., Adeyemo, A., Cooper, R., Ward, R., Lander, E.S., Daly, M.J., Altshuler, D., 2002. The structure of haplotype blocks in the human genome. Science 296, 2225–2229.

Global Burden of Disease Study 2013 Collaborators, 2015. Global, regional, and national incidence, prevalence, and years lived with disability for 301 acute and chronic diseases and injuries in 188 countries, 1990-2013: a systematic analysis for the Global Burden of Disease Study 2013. Lancet 386, 743–800.

Goff, D.C., Cather, C., Evins, A.E., Henderson, D.C., Freudenreich, O., Copeland, P.M., Bierer, M., Duckworth, K., Sacks, F.M., 2005. Medical morbidity and mortality in schizophrenia: guidelines for psychiatrists. J. Clin. Psychiatry 66, 183–194 quiz 147, 273-274.

Goulding, D.R., Nikolova, V.D., Mishra, L., Zhuo, L., Kimata, K., McBride, S.J., Moy, S.S., Harry, G.J., Garantziotis, S., 2019. Inter-alpha-inhibitor deficiency in the mouse is associated with alterations in anxiety-like behavior, exploration and social approach. Gene Brain Behav. 18, e12505.

Himmelfarb, M., Klopocki, E., Grube, S., Staub, E., Klaman, I., Hinzmann, B., Kristiansen, G., Rosenthal, A., Durst, M., Dahl, E., 2004. ITIH5, a novel member of the inter-alpha-trypsin inhibitor heavy chain family is downregulated in breast cancer. Cancer Lett. 204, 69–77.

Ishii, K., Kubo, K.I., Nakajima, K., 2016. Reelin and neuropsychiatric disorders. Front. Cell. Neurosci. 10, 229.

Ishizuka, K., Kamiya, A., Oh, E.C., Kanki, H., Seshadri, S., Robinson, J.F., Murdoch, H., Dunlop, A.J., Kubo, K., Furukori, K., Huang, B., Zeledon, M., Hayashi-Takagi, A., Okano, H., Nakajima, K., Houslay, M.D., Katsanis, N., Sawa, A., 2011. DISC1-dependent switch from progenitor proliferation to migration in the developing cortex. Nature 473, 92–96.

Jaffe, A.E., Straub, R.E., Shin, J.H., Tao, R., Gao, Y., Collado-Torres, L., Kam-Thong, T., Xi, H.S., Quan, J., Chen, Q., Colantuoni, C., Ulrich, W.S., Maher, B.J., Deep-Soboslay, A., Cross, A.J., Brandon, N.J., Leek, J.T., Hyde, T.M., Kleinman, J.E., Weinberger, D.R., 2018. Developmental and genetic regulation of the human cortex transcriptome illuminate schizophrenia pathogenesis. Nat. Neurosci. 21, 1117–1125.

Kim, D., Langmead, B., Salzberg, S.L., 2015. HISAT: a fast spliced aligner with low memory requirements. Nat. Methods 12, 357–360.

Kirov, G., Rujescu, D., Ingason, A., Collier, D.A., O'Donovan, M.C., Owen, M.J., 2009. Neurexin 1 (NRXN1) deletions in schizophrenia. Schizophr. Bull. 35, 851–854.

Kong, H., Fan, Y., Xie, J., Ding, J., Sha, L., Shi, X., Sun, X., Hu, G., 2008. AQP4 knockout impairs proliferation, migration and neuronal differentiation of adult neural stem cells. J. Cell Sci. 121, 4029–4036.

Lewis, C.M., Levinson, D.F., Wise, L.H., DeLisi, L.E., Straub, R.E., Hovatta, I., Williams, N.M., Schwab, S.G., Pulver, A.E., Faraone, S.V., Brzustowicz, L.M., Kaufmann, C.A., Garver, D.L., Gurling, H.M., Lindholm, E., Coon, H., Moises, H.W., Byerley, W., Shaw, S.H., Mesen, A., Sherrington, R., O'Neill, F.A., Walsh, D., Kendler, K.S., Ekelund, J., Paunio, T., Lonnqvist, J., Peltonen, L., O'Donovan, M.C., Owen, M.J., Wildenauer, D.B., Maier, W., Nestadt, G., Blouin, J.L., Antonarakis, S.E., Mowry, B.J., Silverman, J.M., Crowe, R.R., Cloninger, C.R., Tsuang, M.T., Malaspina, D., Harkavy-Friedman, J.M., Svrakic, D.M., Bassett, A.S., Holcomb, J., Kalsi, G., McQuillin, A., Brynjolfson, J., Sigmundsson, T., Petursson, H., Jazin, E., Zoega, T., Helgason, T., 2003. Genome scan meta-analysis of schizophrenia and bipolar disorder, part II: Schizophrenia. Am. J. Hum. Genet. 73, 34–48.

Li, J.Y., Liu, J., Manaph, N.P.A., Bobrovskaya, L., Zhou, X.F., 2017a. ProBDNF inhibits proliferation, migration and differentiation of mouse neural stem cells. Brain Res. 1668, 46–55.

Li, M., Luo, X.J., Xiao, X., Shi, L., Liu, X.Y., Yin, L.D., Diao, H.B., Su, B., 2011. Allelic differences between Han Chinese and Europeans for functional variants in ZNF804A and their association with schizophrenia. Am. J. Psychiatr. 168, 1318–1325.

Li, M., Wu, D.D., Yao, Y.G., Huo, Y.X., Liu, J.W., Su, B., Chasman, D.I., Chu, A.Y., Huang, T., Qi, L., Zheng, Y., Luo, X.J., 2016. Recent positive selection drives the expansion of a schizophrenia risk nonsynonymous variant at SLC39A8 in Europeans. Schizophr. Bull. 42, 178–190.

Li, X., Luo, Z., Gu, C., Hall, L.S., McIntosh, A.M., Zeng, Y., Porteous, D.J., Hayward, C., Li, M., Yao, Y.G., Zhang, C., Luo, X.J., The 23andme Research Team, 2018. Common variants on 6q16.2, 12q24.31 and 16p13.3 are associated with major depressive disorder. Neuropsychopharmacology 43, 2146–2153.

Li, Z., Chen, J., Yu, H., He, L., Xu, Y., Zhang, D., Yi, Q., Li, C., Li, X., Shen, J., Song, Z., Ji, W., Wang, M., Zhou, J., Chen, B., Liu, Y., Wang, J., Wang, P., Yang, P., Wang, Q., Feng, G., Liu, B., Sun, W., Li, B., He, G., Li, W., Wan, C., Xu, Q., Wen, Z., Liu, K., Huang, F., Ji, J., Ripke, S., Yue, W., Sullivan, P.F., O'Donovan, M.C., Shi, Y., 2017b. Genome-wide association analysis identifies 30 new susceptibility loci for schizophrenia. Nat. Genet. 49, 1576–1583.

Li, Z., Xiang, Y., Chen, J., Li, Q., Shen, J., Liu, Y., Li, W., Xing, Q., Wang, Q., Wang, L., Feng, G., He, L., Zhao, X., Shi, Y., 2015. Loci with genome-wide associations with schizophrenia in the Han Chinese population. Br. J. Psychiatry 207, 490–494.

Liu, J., Li, M., Luo, X.J., Su, B., 2018. Systems-level analysis of risk genes reveals the modular nature of schizophrenia. Schizophr. Res. 201, 261–269.

Livak, K.J., Schmittgen, T.D., 2001. Analysis of relative gene expression data using real-time quantitative PCR and the 2(-Delta Delta C(T)) Method. Methods 25, 402–408.

Love, M.I., Huber, W., Anders, S., 2014. Moderated estimation of fold change and dispersion for RNA-seq data with DESeq2. Genome Biol. 15, 550.

Luo, X.J., Diao, H.B., Wang, J.K., Zhang, H., Zhao, Z.M., Su, B., 2008. Association of haplotypes spanning PDZ-GEF2, LOC728637 and ACSL6 with schizophrenia in Han Chinese. J. Med. Genet. 45, 818–826.

Luo, X.J., Mattheisen, M., Li, M., Huang, L., Rietschel, M., Borglum, A.D., Als, T.D., van den Oord, E.J., Aberg, K.A., Mors, O., Mortensen, P.B., Luo, Z., Degenhardt, F., Cichon, S., Schulze, T.G., Nothen, M.M., Su, B., Zhao, Z., Gan, L., Yao, Y.G., 2015. Systematic integration of brain eQTL and GWAS identifies *ZNF323* as a novel schizophrenia risk gene and suggests recent positive selection based on compensatory advantage on pulmonary function. Schizophr. Bull. 41, 1294–1308.

Ma, L., Tang, J., Wang, D., Zhang, W., Liu, W., Liu, X.H., Gong, W., Yao, Y.G., Chen, X., 2013. Evaluating risk loci for schizophrenia distilled from genome-wide association studies in Han Chinese from Central China. Mol. Psychiatr. 18, 638–639.

Ma, P., Zhao, S., Zeng, W., Yang, Q., Li, C., Lv, X., Zhou, Q., Mao, B., 2011. Xenopus Dbx2 is involved in primary neurogenesis and early neural plate patterning. Biochem. Biophys. Res. Commun. 412, 170–174.

Mao, Y., Ge, X., Frank, C.L., Madison, J.M., Koehler, A.N., Doud, M.K., Tassa, C., Berry, E.M., Soda, T., Singh, K.K., Biechele, T., Petryshen, T.L., Moon, R.T., Haggarty, S.J., Tsai, L.H., 2009. Disrupted in schizophrenia 1 regulates neuronal progenitor proliferation via modulation of GSK3beta/beta-catenin signaling. Cell 136, 1017–1031.

Miyake, Y., Tanaka, K., Arakawa, M., 2018. ITIH3 and ITIH4 polymorphisms and depressive symptoms during pregnancy in Japan: the Kyushu Okinawa maternal and child health study. J. Neural. Transm. 125, 1503–1509.

Ng, M.Y., Levinson, D.F., Faraone, S.V., Suarez, B.K., DeLisi, L.E., Arinami, T., Riley, B., Paunio, T., Pulver, A.E., Irmansyah, Holmans, P.A., Escamilla, M., Wildenauer, D.B., Williams, N.M., Laurent, C., Mowry, B.J., Brzustowicz, L.M., Maziade, M., Sklar, P., Garver, D.L., Abecasis, G.R., Lerer, B., Fallin, M.D., Gurling, H.M., Gejman, P.V., Lindholm, E., Moises, H.W., Byerley, W., Wijsman, E.M., Forabosco, P., Tsuang, M.T., Hwu, H.G., Okazaki, Y., Kendler, K.S., Wormley, B., Fanous, A., Walsh, D., O'Neill, F.A., Peltonen, L., Nestadt, G., Lasseter, V.K., Liang, K.Y., Papadimitriou, G.M., Dikeos, D.G., Schwab, S.G., Owen, M.J., O'Donovan, M.C., Norton, N., Hare, E., Raventos, H., Nicolini, H., Albus, M., Maier, W., Nimgaonkar, V.L., Terenius, L., Mallet, J., Jay, M., Godard, S., Nertney, D., Alexander, M., Crowe, R.R., Silverman, J.M., Bassett, A.S., Roy, M.A., Merette, C., Pato, C.N., Pato, M.T., Roos, J.L., Kohn, Y., Amann-Zalcenstein, D., Kalsi, G., McQuillin, A., Curtis, D., Brynjolfson, J., Sigmundsson, T., Petursson, H., Sanders, A.R., Duan, J., Jazin, E., Myles-Worsley, M., Karayiorgou, M., Lewis, C.M., 2009. Meta-analysis of 32 genome-wide linkage studies of schizophrenia. Mol. Psychiatr. 14, 774–785.

O'Donovan, M.C., Craddock, N., Norton, N., Williams, H., Peirce, T., Moskvina, V., Nikolov, I., Hamshere, M., Carroll, L., Georgieva, L., Dwyer, S., Holmans, P., Marchini, J.L., Spencer, C.C., Howie, B., Leung, H.T., Hartmann, A.M., Moller, H.J., Morris, D.W., Shi, Y., Feng, G., Hoffmann, P., Propping, P., Vasilescu, C., Maier, W., Rietschel, M., Zammit, S., Schumacher, J., Quinn, E.M., Schulze, T.G., Williams, N.M., Giegling, I., Iwata, N., Ikeda, M., Darvasi, A., Shifman, S., He, L., Duan, J., Sanders, A.R., Levinson, D.F., Gejman, P.V., Cichon, S., Nothen, M.M., Gill, M., Corvin, A., Rujescu, D., Kirov, G., Owen, M.J., Buccola, N.G., Mowry, B.J., Freedman, R., Amin, F., Black, D.W., Silverman, J.M., Byerley, W.F., Cloninger, C.R., 2008. Identification of loci associated with schizophrenia by genome-wide association and follow-up. Nat. Genet. 40, 1053–1055.

Oakley, P., Kisely, S., Baxter, A., Harris, M., Desoe, J., Dziouba, A., Siskind, D., 2018. Increased mortality among people with schizophrenia and other non-affective psychotic disorders in the community: a systematic review and meta-analysis. J. Psychiatr. Res. 102, 245–253.

Owen, M.J., O'Donovan, M.C., Thapar, A., Craddock, N., 2011. Neurodevelopmental hypothesis of schizophrenia. Br. J. Psychiatry 198, 173–175.

Owen, M.J., Sawa, A., Mortensen, P.B., 2016. Schizophrenia. Lancet 388, 86–97.
Palmer, B.A., Pankratz, V.S., Bostwick, J.M., 2005. The lifetime risk of suicide in schizophrenia: a reexamination. Arch. Gen. Psychiatr. 62, 247–253.
Pardinas, A.F., Holmans, P., Pocklington, A.J., Escott-Price, V., Ripke, S., Carrera, N., Legge, S.E., Bishop, S., Cameron, D., Hamshere, M.L., Han, J., Hubbard, L., Lynham, A., Mantripragada, K., Rees, E., MacCabe, J.H., McCarroll, S.A., Baune, B.T., Breen, G., Byrne, E.M., Dannlowski, U., Eley, T.C., Hayward, C., Martin, N.G., McIntosh, A.M., Plomin, R., Porteous, D.J., Wray, N.R., Caballero, A., Geschwind, D.H., Huckins, L.M., Ruderfer, D.M., Santiago, E., Sklar, P., Stahl, E.A., Won, H., Agerbo, E., Als, T.D., Andreassen, O.A., Baekvad-Hansen, M., Mortensen, P.B., Pedersen, C.B., Borglum, A.D., Bybjerg-Grauholm, J., Djurovic, S., Durmishi, N., Pedersen, M.G., Golimbet, V., Grove, J., Hougaard, D.M., Mattheisen, M., Molden, E., Mors, O., Nordentoft, M., Pejovic-Milovancevic, M., Sigurdsson, E., Silagadze, T., Hansen, C.S., Stefansson, K., Stefansson, H., Steinberg, S., Tosato, S., Werge, T., Collier, D.A., Rujescu, D., Kirov, G., Owen, M.J., O'Donovan, M.C., Walters, J.T.R., 2018. Common schizophrenia alleles are enriched in mutation-intolerant genes and in regions under strong background selection. Nat. Genet. 50, 381–389.
Peall, K.J., Dijk, J.M., Saunders-Pullman, R., Dreissen, Y.E., van Loon, I., Cath, D., Kurian, M.A., Owen, M.J., Foncke, E.M., Morris, H.R., Gasser, T., Bressman, S., Asmus, F., Tijssen, M.A., 2015. Psychiatric disorders, myoclonus dystonia and SGCE: an international study. Ann. Clin. Transl. Neurol. 3, 4–11.
Pertea, M., Pertea, G.M., Antonescu, C.M., Chang, T.C., Mendell, J.T., Salzberg, S.L., 2015. StringTie enables improved reconstruction of a transcriptome from RNA-seq reads. Nat. Biotechnol. 33, 290–295.
Psychiatric GWAS Consortium Bipolar Disorder Working Group, 2011. Large-scale genome-wide association analysis of bipolar disorder identifies a new susceptibility locus near *ODZ4*. Nat. Genet. 43, 977–983.
Purcell, S., Neale, B., Todd-Brown, K., Thomas, L., Ferreira, M.A., Bender, D., Maller, J., Sklar, P., de Bakker, P.I., Daly, M.J., Sham, P.C., 2007. PLINK: a tool set for whole-genome association and population-based linkage analyses. Am. J. Hum. Genet. 81, 559–575.
Randhawa, P.K., Rylova, S., Heinz, J.Y., Kiser, S., Fried, J.H., Dunworth, W.P., Anderson, A.L., Barber, A.T., Chappell, J.C., Roberts, D.M., Bautch, V.L., 2011. The Ras activator RasGRP3 mediates diabetes-induced embryonic defects and affects endothelial cell migration. Circ. Res. 108, 1199–1208.
Saha, S., Chant, D., McGrath, J., 2007. A systematic review of mortality in schizophrenia: is the differential mortality gap worsening over time? Arch. Gen. Psychiatr. 64, 1123–1131.
Saha, S., Chant, D., Welham, J., McGrath, J., 2005. A systematic review of the prevalence of schizophrenia. PLoS Med. 2, e141.
Schizophrenia Psychiatric Genome-Wide Association Study (GWAS) Consortium, 2011. Genome-wide association study identifies five new schizophrenia loci. Nat. Genet. 43, 969–976.
Schizophrenia Working Group of the Psychiatric Genomics Consortium, 2014. Biological insights from 108 schizophrenia-associated genetic loci. Nature 511, 421–427.
Senturk, A., Pfennig, S., Weiss, A., Burk, K., Acker-Palmer, A., 2011. Ephrin Bs are essential components of the Reelin pathway to regulate neuronal migration. Nature 472, 356–360.
Shi, Y., Li, Z., Xu, Q., Wang, T., Li, T., Shen, J., Zhang, F., Chen, J., Zhou, G., Ji, W., Li, B., Xu, Y., Liu, D., Wang, P., Yang, P., Liu, B., Sun, W., Wan, C., Qin, S., He, G., Steinberg, S., Cichon, S., Werge, T., Sigurdsson, E., Tosato, S., Palotie, A., Nothen, M.M., Rietschel, M., Ophoff, R.A., Collier, D.A., Rujescu, D., Clair, D.S., Stefansson, H., Stefansson, K., Ji, J., Wang, Q., Li, W., Zheng, L., Zhang, H., Feng, G., He, L., 2011. Common variants on 8p12 and 1q24.2 confer risk of schizophrenia. Nat. Genet. 43, 1224–1227.
Sullivan, P.F., Kendler, K.S., Neale, M.C., 2003. Schizophrenia as a complex trait: evidence from a meta-analysis of twin studies. Arch. Gen. Psychiatr. 60, 1187–1192.
The 1000 Genomes Project Consortium, 2015. A global reference for human genetic variation. Nature 526, 68–74.
The GTEx Consortium, 2015. The Genotype-Tissue Expression (GTEx) pilot analysis: multitissue gene regulation in humans. Science 348, 648–660.
Ullrich, B., Li, C., Zhang, J.Z., McMahon, H., Anderson, R.G., Geppert, M., Sudhof, T.C., 1994. Functional properties of multiple synaptotagmins in brain. Neuron 13, 1281–1291.
Walker, E., Kestler, L., Bollini, A., Hochman, K.M., 2004. Schizophrenia: etiology and course. Annu. Rev. Psychol. 55, 401–430.
Walsh, T., McClellan, J.M., McCarthy, S.E., Addington, A.M., Pierce, S.B., Cooper, G.M., Nord, A.S., Kusenda, M., Malhotra, D., Bhandari, A., Stray, S.M., Rippey, C.F., Roccanova, P., Makarov, V., Lakshmi, B., Findling, R.L., Sikich, L., Stromberg, T., Merriman, B., Gogtay, N., Butler, P., Eckstrand, K., Noory, L., Gochman, P., Long, R., Chen, Z., Davis, S., Baker, C., Eichler, E.E., Meltzer, P.S., Nelson, S.F., Singleton, A.B., Lee, M.K., Rapoport, J.L., King, M.C., Sebat, J., 2008. Rare structural variants disrupt multiple genes in neurodevelopmental pathways in schizophrenia. Science 320, 539–543.
Whittaker, C.A., Hynes, R.O., 2002. Distribution and evolution of von Willebrand/integrin A domains: widely dispersed domains with roles in cell adhesion and elsewhere. Mol. Biol. Cell 13, 3369–3387.
Windrem, M.S., Osipovitch, M., Liu, Z., Bates, J., Chandler-Militello, D., Zou, L., Munir, J., Schanz, S., McCoy, K., Miller, R.H., Wang, S., Nedergaard, M., Findling, R.L., Tesar, P.J., Goldman, S.A., 2017. Human iPSC glial mouse chimeras reveal glial contributions to schizophrenia. Cell Stem Cell 21, 195–208 e6.
Won, S.J., Kim, S.H., Xie, L., Wang, Y., Mao, X.O., Jin, K., Greenberg, D.A., 2006. Reelin-deficient mice show impaired neurogenesis and increased stroke size. Exp. Neurol. 198, 250–259.
Yang, C.P., Li, X., Wu, Y., Shen, Q., Zeng, Y., Xiong, Q., Wei, M., Chen, C., Liu, J., Huo, Y., Li, K., Xue, G., Yao, Y.G., Zhang, C., Li, M., Chen, Y., Luo, X.J., 2018. Comprehensive integrative analyses identify *GLT8D1* and *CSNK2B* as schizophrenia risk genes. Nat. Commun. 9, 838.
Yang, Z., Zhou, D., Li, H., Cai, X., Liu, W., Wang, L., Chang, H., Li, M., Xiao, X., 2019. The genome-wide risk alleles for psychiatric disorders at 3p21.1 show convergent effects on mRNA expression, cognitive function, and mushroom dendritic spine. Mol. Psychiatr. 25, 48–66.
Yu, G.C., Wang, L.G., Han, Y.Y., He, Q.Y., 2012. clusterProfiler: an R Package for comparing biological themes among gene clusters. Omics 16, 284–287.
Yu, H., Yan, H., Li, J., Li, Z., Zhang, X., Ma, Y., Mei, L., Liu, C., Cai, L., Wang, Q., Zhang, F., Iwata, N., Ikeda, M., Wang, L., Lu, T., Li, M., Xu, H., Wu, X., Liu, B., Yang, J., Li, K., Lv, L., Ma, X., Wang, C., Li, L., Yang, F., Jiang, T., Shi, Y., Li, T., Zhang, D., Yue, W., 2017. Common variants on 2p16.1, 6p22.1 and 10q24.32 are associated with schizophrenia in Han Chinese population. Mol. Psychiatr. 22, 954–960.
Yue, W.H., Wang, H.F., Sun, L.D., Tang, F.L., Liu, Z.H., Zhang, H.X., Li, W.Q., Zhang, Y.L., Zhang, Y., Ma, C.C., Du, B., Wang, L.F., Ren, Y.Q., Yang, Y.F., Hu, X.F., Wang, Y., Deng, W., Tan, L.W., Tan, Y.L., Chen, Q., Xu, G.M., Yang, G.G., Zuo, X.B., Yan, H., Ruan, Y.Y., Lu, T.L., Han, X., Ma, X.H., Cai, L.W., Jin, C., Zhang, H.Y., Yan, J., Mi, W.F., Yin, X.Y., Ma, W.B., Liu, Q., Kang, L., Sun, W., Pan, C.Y., Shuang, M., Yang, F.D., Wang, C.Y., Yang, J.L., Li, K.Q., Ma, X., Li, L.J., Yu, X., Li, Q.Z., Huang, X., Lv, L.X., Li, T., Zhao, G.P., Huang, W., Zhang, X.J., Zhang, D., 2011. Genome-wide association study identifies a susceptibility locus for schizophrenia in Han Chinese at 11p11.2. Nat. Genet. 43, 1228–1231.
Zhang, W., Xiao, M.S., Ji, S., Tang, J., Xu, L., Li, X., Li, M., Wang, H.Z., Jiang, H.Y., Zhang, D.F., Wang, J., Zhang, S., Xu, X.F., Yu, L., Zheng, P., Chen, X., Yao, Y.G., 2014. Promoter variant rs2301228 on the neural cell adhesion molecule 1 gene confers risk of schizophrenia in Han Chinese. Schizophr. Res. 160, 88–96.

Supplementary Data

Table S1：Results of the Hardy-Weinberg equilibrium test of the genotyped SNPs

SNP	CHR	TEST	A1/A2	GENO	O(HET)	E(HET)	P
rs3176443	1	ALL	G/C	424/3768/9135	0.2827	0.2864	0.1465
rs3176443	1	AFF	G/C	125/1154/2811	0.2822	0.2844	0.6207
rs3176443	1	UNAFF	G/C	299/2614/6324	0.2830	0.2873	0.1577
rs3617	3	ALL	A/C	2538/6398/4408	0.4795	0.4902	0.0116
rs3617	3	AFF	A/C	656/1889/1527	0.4639	0.4771	0.0762
rs3617	3	UNAFF	A/C	1882/4509/2881	0.4863	0.4942	0.1250
rs3774729	3	ALL	G/A	3210/6679/3469	0.5000	0.4998	0.9724
rs3774729	3	AFF	G/A	1020/2058/1012	0.5032	0.5000	0.7075
rs3774729	3	UNAFF	G/A	2190/4621/2457	0.4986	0.4996	0.8516
rs950169	15	ALL	T/C	58/1568/11703	0.1176	0.1184	0.4643
rs950169	15	AFF	T/C	13/480/3572	0.1181	0.1167	0.5896
rs950169	15	UNAFF	T/C	45/1088/8131	0.1174	0.1191	0.1900
rs4584886	17	ALL	C/T	225/2967/10175	0.2220	0.2230	0.6140
rs4584886	17	AFF	C/T	72/884/3142	0.2157	0.2194	0.2853
rs4584886	17	UNAFF	C/T	153/2083/7033	0.2247	0.2245	0.9631
rs2288920	19	ALL	T/G	557/4313/8401	0.3250	0.3253	0.9150
rs2288920	19	AFF	T/G	143/1298/2572	0.3234	0.3168	0.1952
rs2288920	19	UNAFF	T/G	414/3015/5829	0.3257	0.3289	0.3432
rs20551	22	ALL	G/A	88/1851/11305	0.1398	0.1413	0.1966

rs20551	22	AFF	G/A	26/585/3374	0.1468	0.1471	0.9140
rs20551	22	UNAFF	G/A	62/1266/7931	0.1367	0.1389	0.1543
rs133335	22	ALL	A/G	362/3484/9359	0.2638	0.2679	0.0851
rs133335	22	AFF	A/G	93/1018/2825	0.2586	0.2591	0.9021
rs133335	22	UNAFF	A/G	269/2466/6534	0.2660	0.2716	0.0511

Abbreviations: SNP, single nucleotide polymorphism; CHR, chromosome; TEST, type of test; A1, minor allele; A2, major allele; GENO, genotype counts: A1A1/A1A2/A2A2; O(HET), observed heterozygosity; E(HET), expected heterozygosity; P, p value.

Table S2: The association significance of the studied coding SNPs in Chinese and European populations

SNP	CHR:BP	A1	A2	P	OR	A1 (CLOZUK+PGC)	A2 (CLOZUK+PGC)	P (CLOZUK+PGC)	OR (CLOZUK+PGC)
rs3176443	1:177247854	G	C	7.15E-01	0.987	G	C	2.84E-07	1.064
rs3774729	3:63982082	G	A	1.48E-02	1.067	G	A	1.37E-08	0.944
rs3617	**3:52833805**	**A**	**C**	**8.36E-16**	**0.803**	**A**	**C**	**1.01E-11**	**0.937**
rs950169	15:84706461	T	C	6.80E-01	0.978	T	C	5.00E-09	0.938
rs4584886	17:17896205	C	T	4.68E-01	0.971	C	T	7.37E-07	0.951
rs2288920	19:50091798	T	G	7.82E-02	0.943	T	G	7.71E-09	0.929
rs133335	22:42416056	A	G	6.98E-02	0.935	A	G	5.72E-10	0.943
rs20551	22:41548008	G	A	1.74E-01	1.070	G	A	1.30E-09	1.066

Abbreviations: SNP, single nucleotide polymorphism; CHR, chromosome; BP, base-pair position; A1, effect allele; A2, alternative allele; P, p value; OR, odds ratio (based on A1 allele); CLOZUK+PGC, GWAS study from the Pardinas *et al* (2018) (Nature Genetics).

Table S3: Meta analysis of the significant non-synonymous SNP rs3617

SNP	CHR:BP	A1	A2	P	OR	P(CLOZUK+PGC)	OR(CLOZUK+PGC)	P(meta)	OR(meta)
rs3617	3:52833805	A	C	8.36E-16	0.803	1.01E-11	0.937	1.35E-19	0.922

Abbreviations: SNP, single nucleotide polymorphism; CHR, chromosome; BP, base-pair position; A1, effect allele; A2, alternative allele; P, p value; OR, odds ratio (for A1 allele); CLOZUK+PGC, GWAS study from the Pardinas *et al* (2018) (Nature Genetics); meta, meta analysis.

Table S4: The associations between rs3617 and gene expression in human brain tissues

SNP Id	Gene Symbol	P-Value	Tissue
rs3617	*GLYCTK*	2.80×10^{-05}	Brain - Anterior cingulate cortex (BA24)
rs3617	*GNL3*	5.10×10^{-09}	Brain - Cerebellar Hemisphere
rs3617	*PPM1M*	4.80×10^{-05}	Brain - Cerebellar Hemisphere
rs3617	*GNL3*	1.20×10^{-11}	Brain - Cerebellum
rs3617	*GLYCTK*	1.60×10^{-06}	Brain - Cerebellum
rs3617	*PPM1M*	9.20×10^{-06}	Brain - Cerebellum
rs3617	*GNL3*	2.20×10^{-05}	Brain - Frontal Cortex (BA9)
rs3617	*GNL3*	1.30×10^{-05}	Brain - Hypothalamus
rs3617	*GNL3*	2.00×10^{-07}	Brain - Putamen (basal ganglia)

Data was from the GTEx website (https://gtexportal.org/home/).

Table S5: The associations between rs3617 and gene expression in human brain tissues

SNP id	Gene symbol	P value	FDR
rs3617	*GNL3*	7.89×10^{-11}	1.63×10^{-8}
rs3617	*NEK4*	1.89×10^{-6}	1.82×10^{-4}

Data was from the LIBD eQTL dataset (the dorsolateral prefrontal cortex of 412 subjects were used for eQTL analysis) (http://eqtl.brainseq.org/phase1/eqtl/)

Table S6. PCR primers used to amplify the genomic sequence containing the test SNP

	Primers (5'-3')	
SNP ID	F (Forward)	R (Reverse)
rs4584886	CTTTCTCCCTTTTTCTCCCC	GCTACTCTTCAATGCCCCTT
rs3617	AGGATAAGAGAAGGCTCACGGC	ACAGAGGGAGGCACCGCTAGGA
rs20551	GCTATCCTGTTGCTTACCTTAC	CAGTGCTTCTCTCTTCTGTTTC
rs3774729	TGAACTGCCTGTCAACTCCCA	TGGGGCTCACAGTCCATTTCC
rs3176443	CTCCACAGCTATCTCCCAGTTC	CTCTCTCACTTCAGACGCAACT
rs950169	CAATGCACTTCTGACTCTCAT	GTTTTTGAATCAGCGACATGG
rs2288920	TTACAGTGGGGTAGGGGTTATG	AGTCGCCAAAACCAGACACAAG
rs133335	AGGTAGTGCTTCCCTTGGTGTT	TAATCTTTGTGTTCCTACCCTG

Table S7: SNaPshot primers used to genotype the test SNP

SNP ID	Extension Primers (5'-3')
rs3176443	TTTTTTTTTTTTTTTTCAAAAAGACCCATCGGATC
rs3617	TTTTTTTTTTTTTTTTTTTCAGAATCCTGGAAGATATG
rs20551	TTTTTTTTTTTTTTTTTTTTTTTTTCCCTACTCTCACCTCTGAAA
rs133335	TTTTTTTTTTTTTTTTTTTTTTTTTTTTTTTTTTTTTTTTATTAGTCTTCAGAAATGGAG
rs950169	TTTTTTTTTTTTTTTTTTTTTTTTTTTTTTTTTTTTTTTTTTTTTCTTTTTTGCAGGAGACTGCA
rs2288920	TTTTTTTTTTTTTTTTTTTTTTTTTTTTTTTTTTTTTTTTTTTTTTTTTTGACAATGAGCAGGATGCCAC
rs3774729	TTTTTTTTTTTTTTTTTTTTTTTTTTTTTTTTTTTTTTTTTTTTTTTTTTTTTTTAGGTTGCCAAAGTGCCAGCC
rs4584886	TTTTTTTTTTTTTTTTTTTTTTTTTTTTTTTTTTTTTTTTTTTTTTTTTTTTTTTTTTTTACCTCATGTACCTGGACTAC

Table S8：The Real-time qPCR primers used in this study

		RT-PCR primers (5'-3')	
Gene	Species	Forward	Reverse
Actin	Mouse	CATGTACGTTGCTATCCAGGC	CTCCTTAATGTCACGCACGAT
Dbx2	Mouse	CCCCGCCATTCTACTCTGC	CGAGCTTTGGAATTTGAGTCCTG
Sgce	Mouse	TCTGACCGGAACGTGTACC	TTGGATAAGGTGGAAATTCACCC
Syt1	Mouse	ACCCTGGGCTCTGTATCCC	CCCTGACCACTGAGTGCAAA
Rasgrp3	Mouse	AACGACAGTTACTTGCCCAGA	CCTCAGTCATGCGAATCAAACC
Peg10	Mouse	TGCTTGCACAGAGCTACAGTC	AGTTTGGGATAGGGGCTGCT

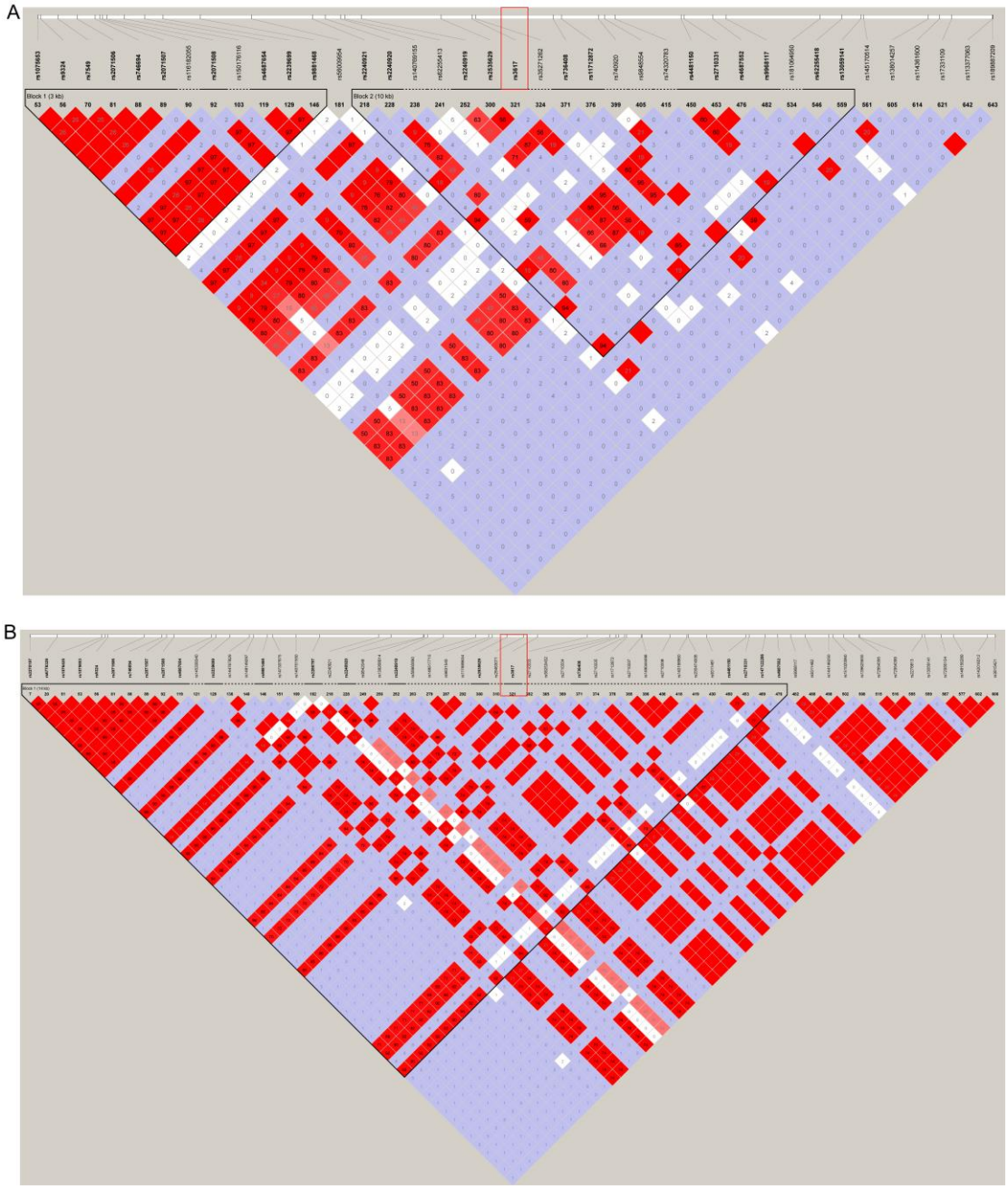

Fig. S1. Linkage disequilibrium patterns of the SNPs surrounding rs3617 in European (CEU) and Chinese (CHB) populations. Genotype data was from the 1000 Genomes project. The LD values were expressed as $r^2 \times 100$.

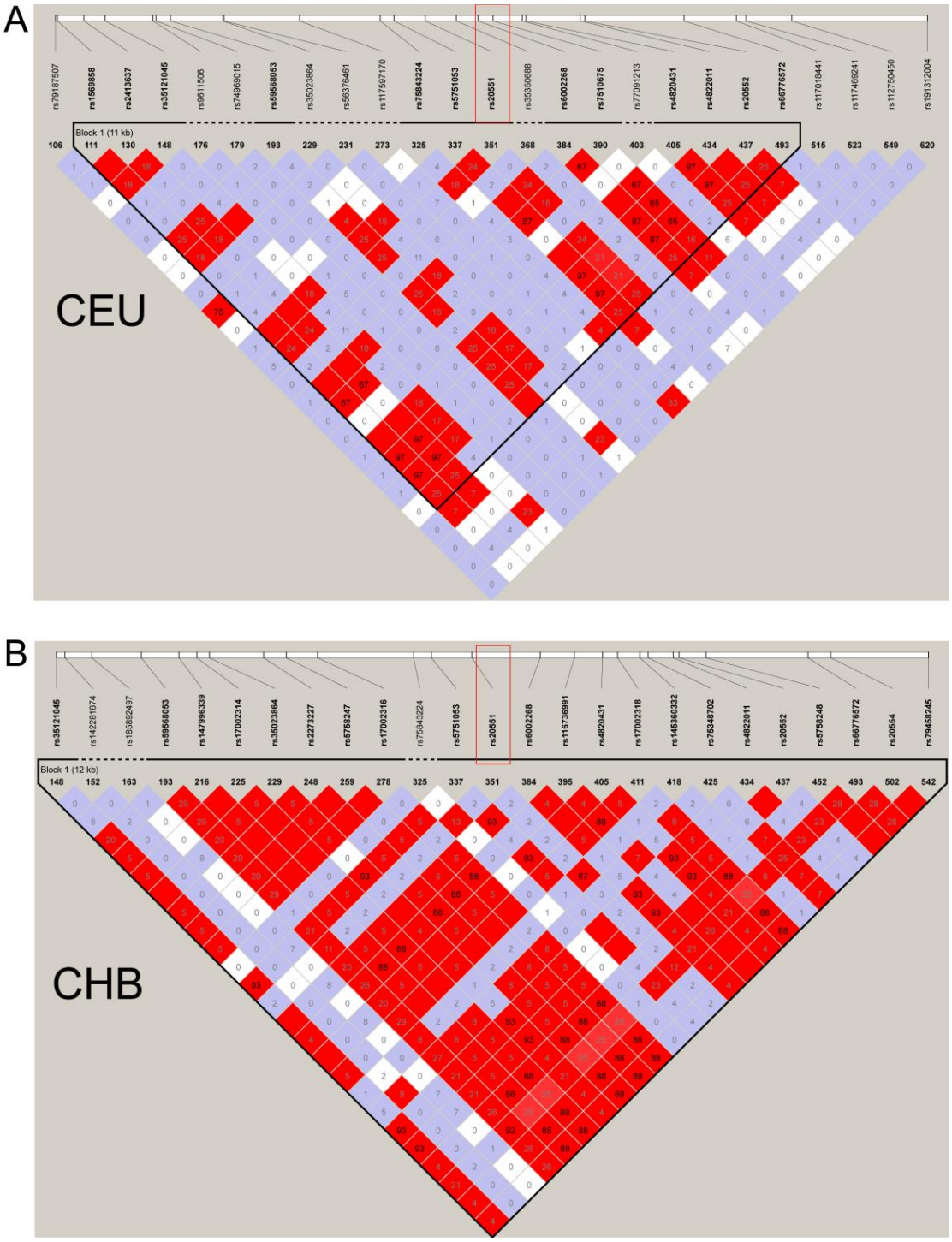

Fig. S2. Linkage disequilibrium patterns of the SNPs surrounding rs20551 in European (CEU) and Chinese (CHB) populations. Genotype data was from the 1000 Genomes project. The LD values were expressed as $r^2 \times 100$.

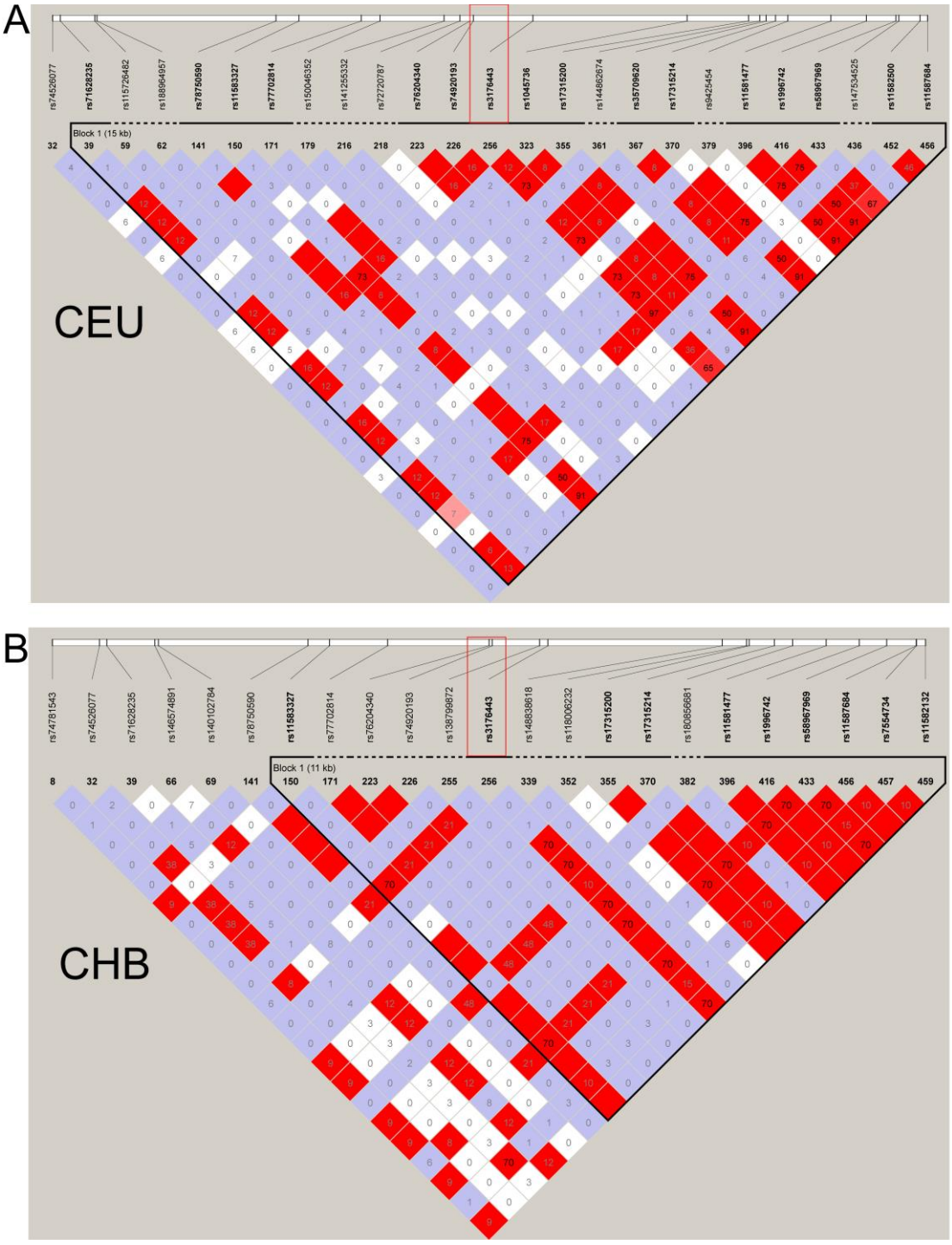

Fig. S3. Linkage disequilibrium patterns of the SNPs surrounding rs3176443 in European (CEU) and Chinese (CHB) populations. Genotype data was from the 1000 Genomes project. The LD values were expressed as $r^2 \times 100$.

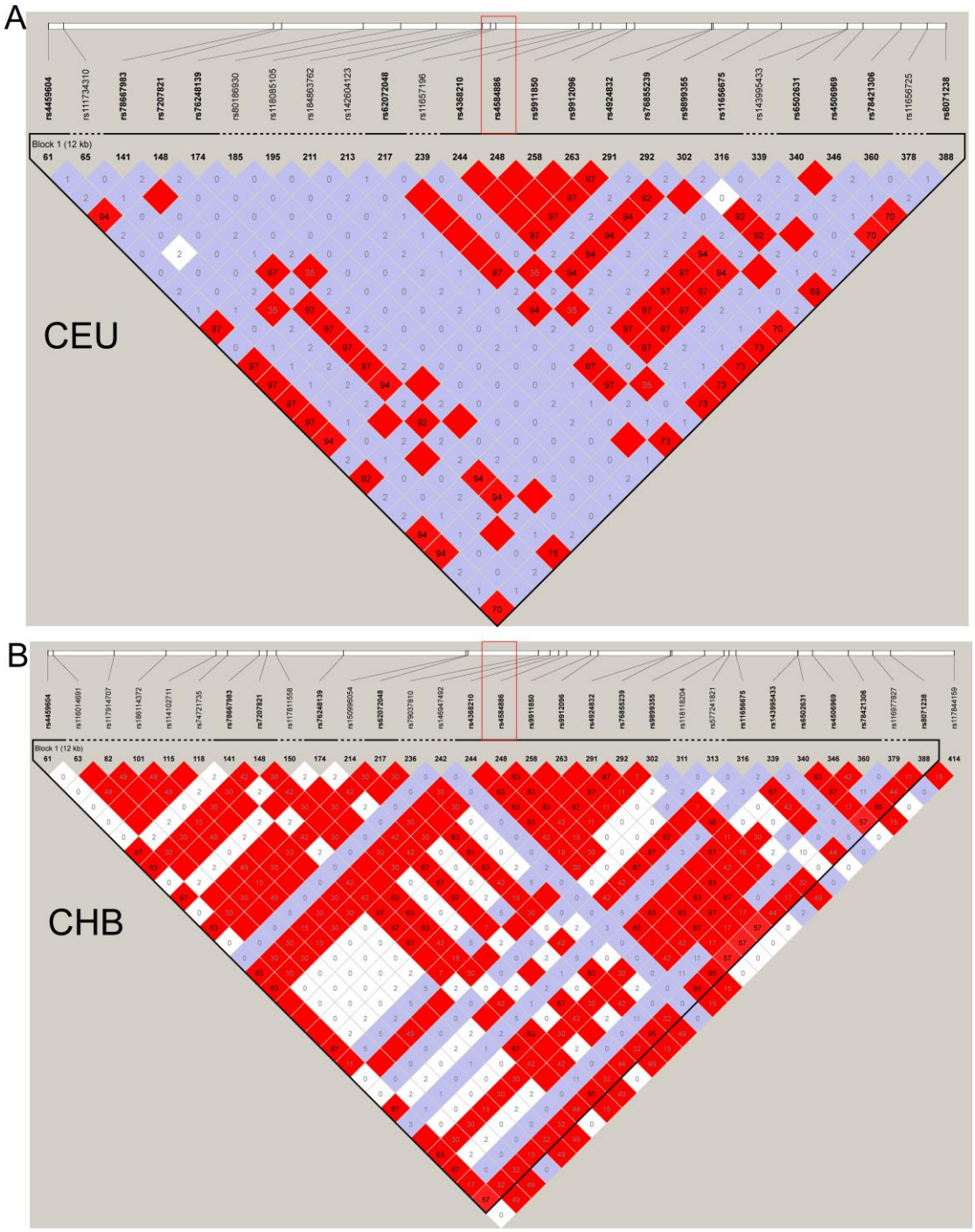

Fig. S4. Linkage disequilibrium patterns of the SNPs surrounding rs4584886 in European (CEU) and Chinese (CHB) populations. Genotype data was from the 1000 Genomes project. The LD values were expressed as $r^2 \times 100$.

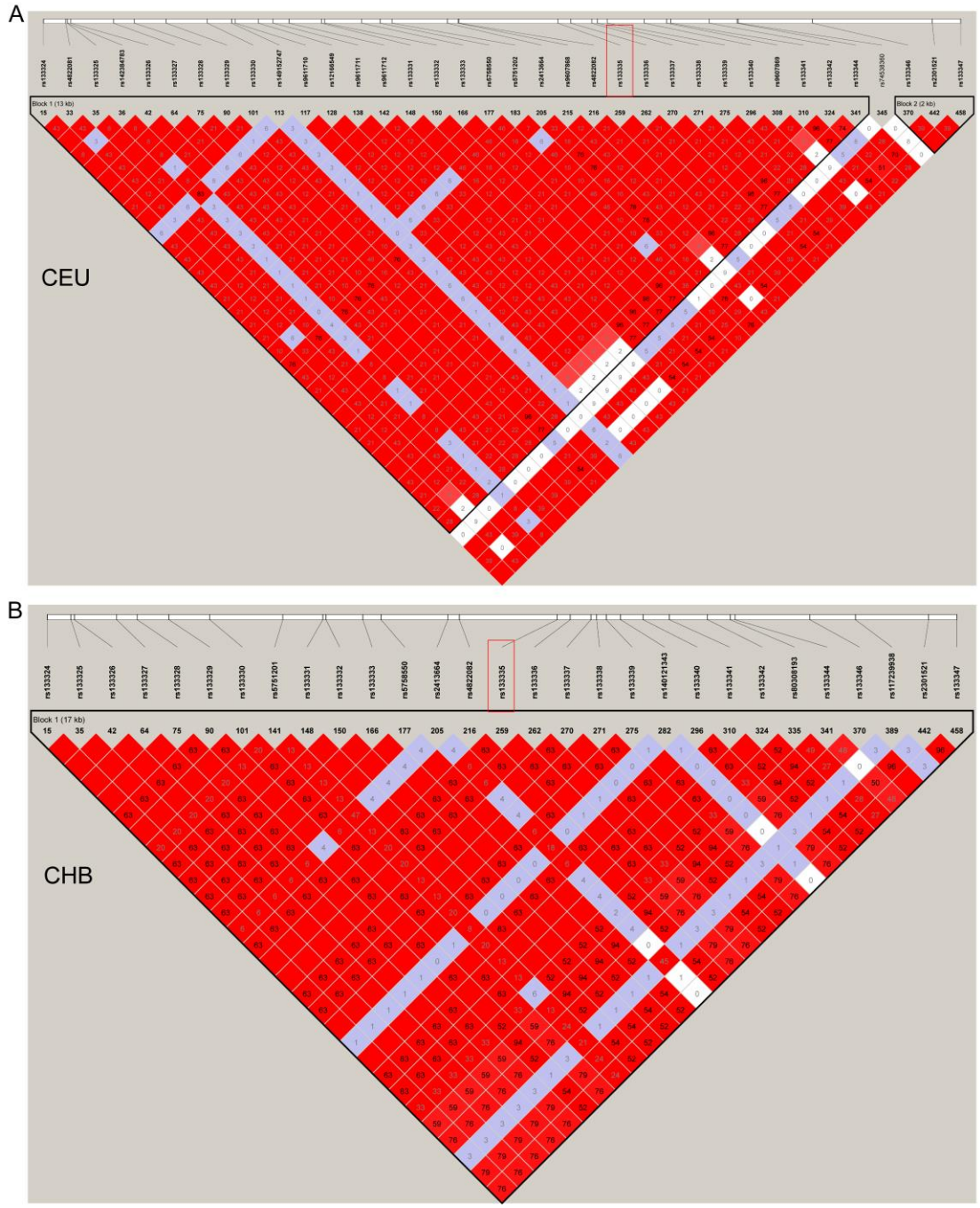

Fig. S5. Linkage disequilibrium patterns of the SNPs surrounding rs133335 in European (CEU) and Chinese (CHB) populations. Genotype data was from the 1000 Genomes project. The LD values were expressed as $r^2 \times 100$.

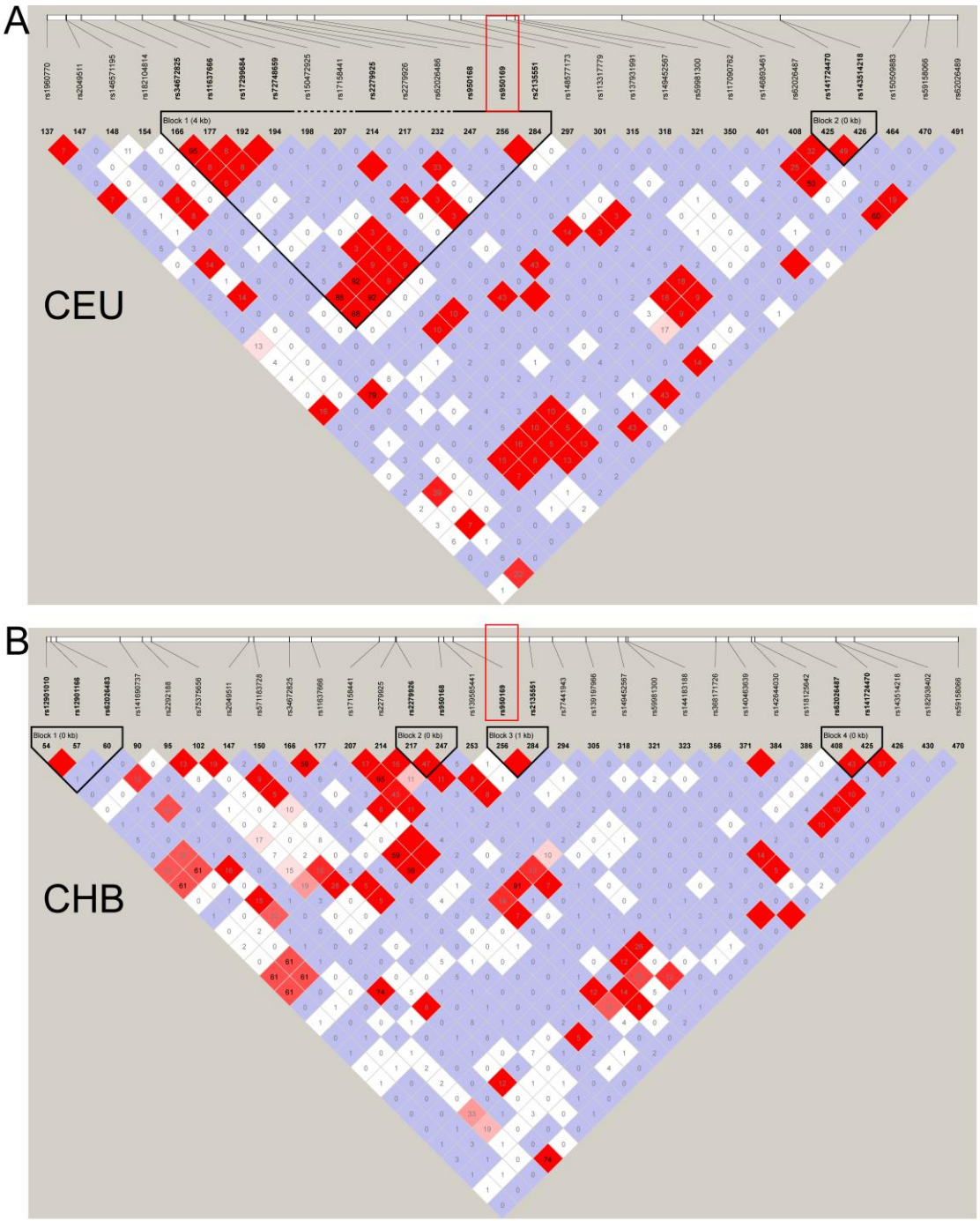

Fig. S6. Linkage disequilibrium patterns of the SNPs surrounding rs950169 in European (CEU) and Chinese (CHB) populations. Genotype data was from the 1000 Genomes project. The LD values were expressed as $r^2 \times 100$.

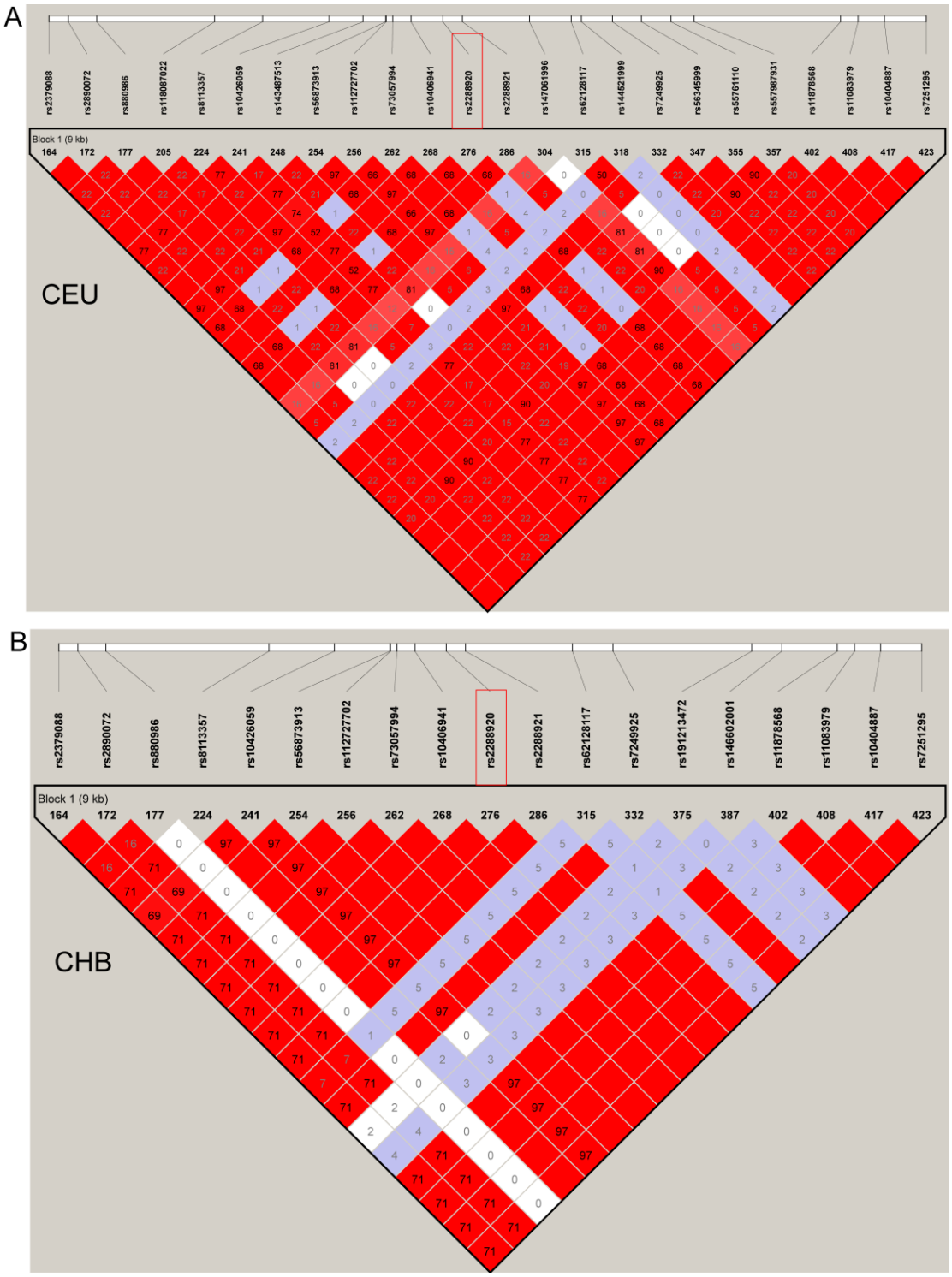

Fig. S7. Linkage disequilibrium patterns of the SNPs surrounding rs2288920 in European (CEU) and Chinese (CHB) populations. Genotype data was from the 1000 Genomes project. The LD values were expressed as $r^2 \times 100$.

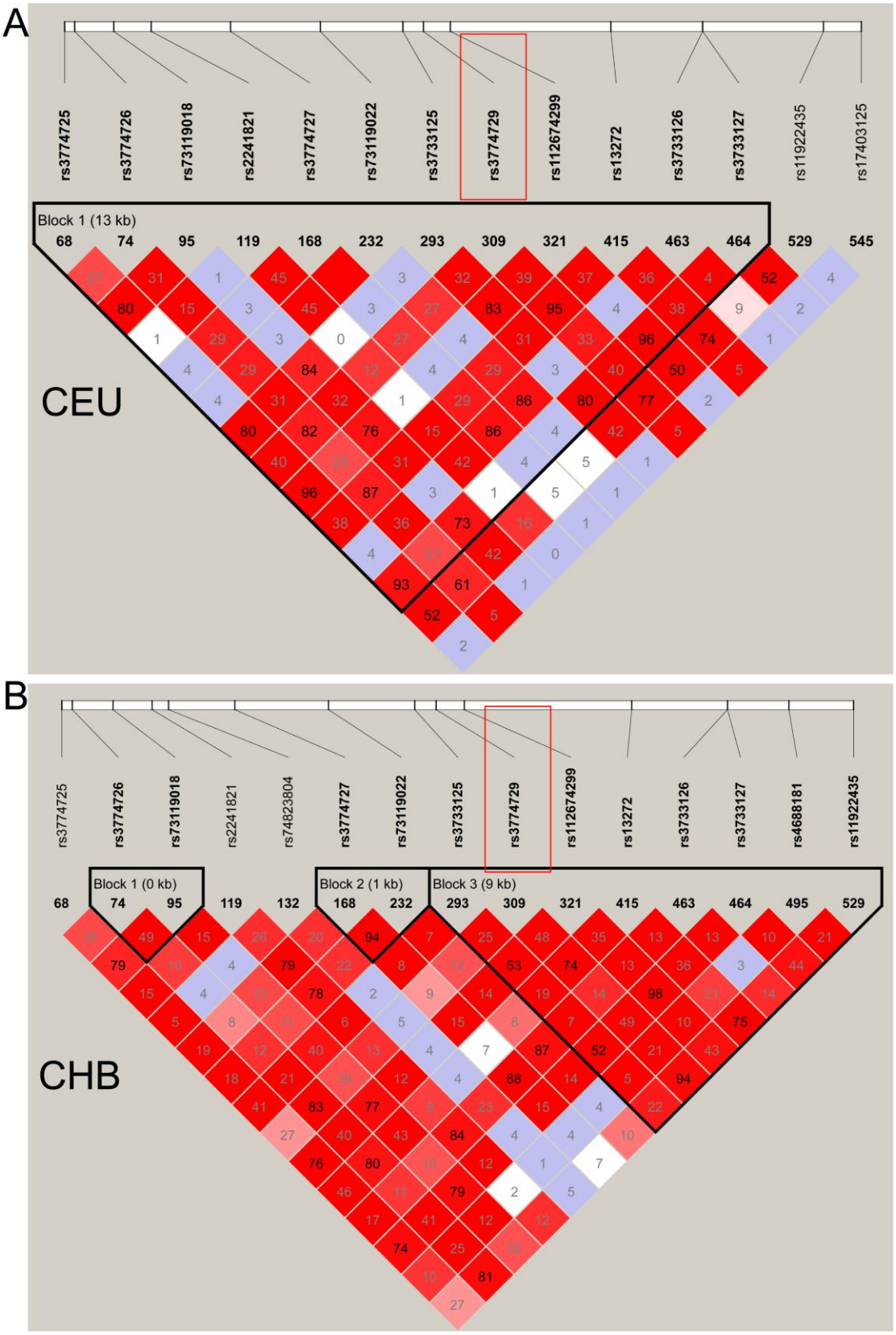

Fig. S8. Linkage disequilibrium patterns of the SNPs surrounding rs3774729 in European (CEU) and Chinese (CHB) populations. Genotype data was from the 1000 Genomes project. The LD values were expressed as $r^2 \times 100$.

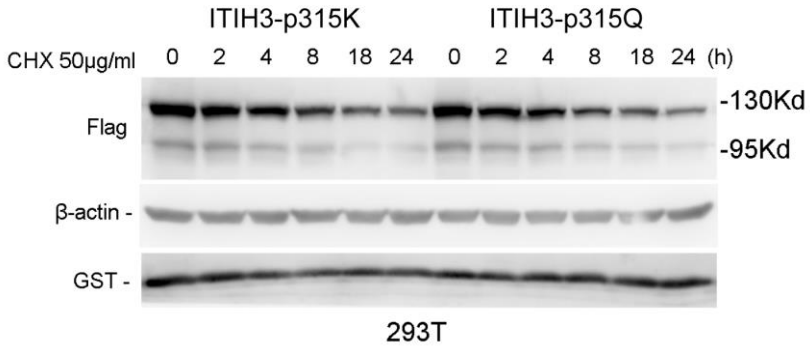

Fig. S9. pK315Q did not affect ITIH3 degradation. HEK293T cells were transfected with ITIH3 expression plasmids containing either A or C at rs3616 (encode lysine and glutamine at the 315 amino acid site, respectively). After treating the cells with cycloheximide (CHX) for the indicated time, the expression of ITIH3 protein was analyzed by WB. GST was detected as transfection efficiency control and β-actin was used as loading control.

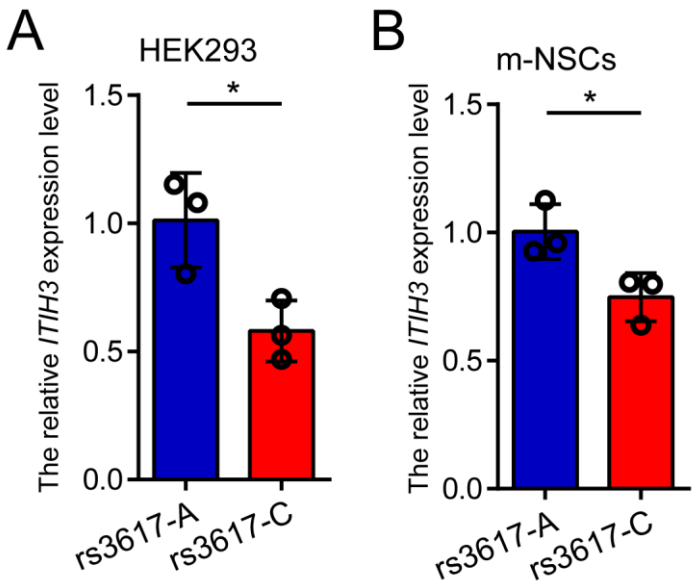

Fig. S10. The C allele of rs3617 is associated lower *ITIH3* mRNA expression. (A) *ITIH3* expression vectors (2.5 μg) containing C (pEGFP-*ITIH3*-C) and A (pEGFP-*ITIH3*-A allele) allele of rs3617 were transiently transfected into HEK293 cells. qPCR was used to quantify *ITIH3* mRNA expression and *ACTIN* was used as internal control. The C allele of rs3617 is associated lower *ITIH3* mRNA expression in HEK293 cells. **(B)** Mouse neural stem cells (NSCs) that stably over-expressing *ITIH3* (with different alleles of rs3617) were used to extract RNA. qPCR was used to quantify *ITIH3* mRNA expression and *Actin* was used as internal control. The C allele of rs3617 is associated lower *ITIH3* mRNA expression in mouse NSCs. Two-tailed *student's t* test was used for statistical test and *P* threshold was set to 0.05. **P*<0.05.

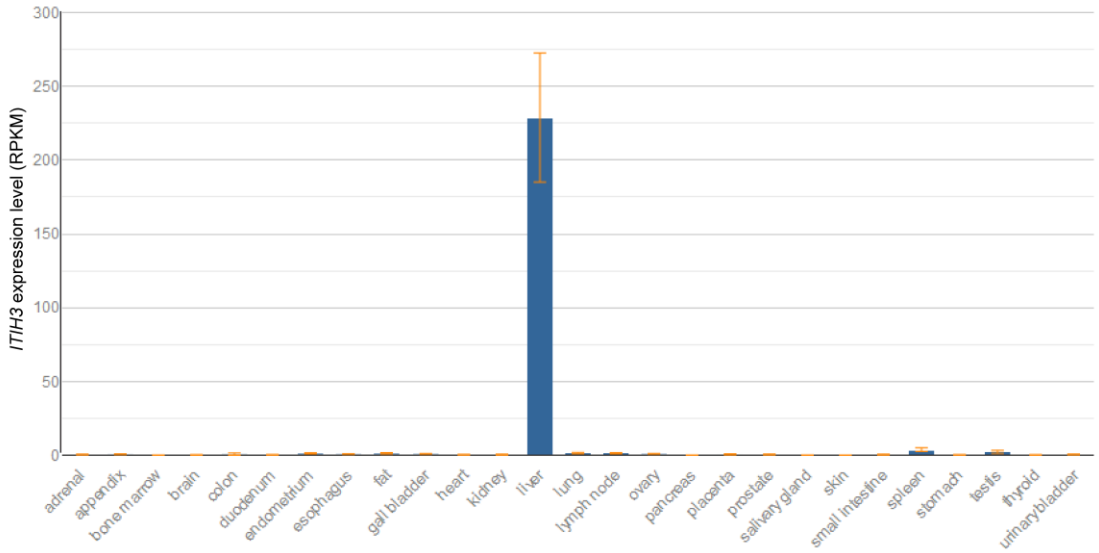

Fig. S11. *ITIH3* expression in different human tissues. *ITIH3* has the highest expression in the liver. In other tissues, expression of *ITIH3* was relatively low. Data from the study of Fagerberg *et al*. [1]. RPKM, reads per kilo base per million mapped reads.

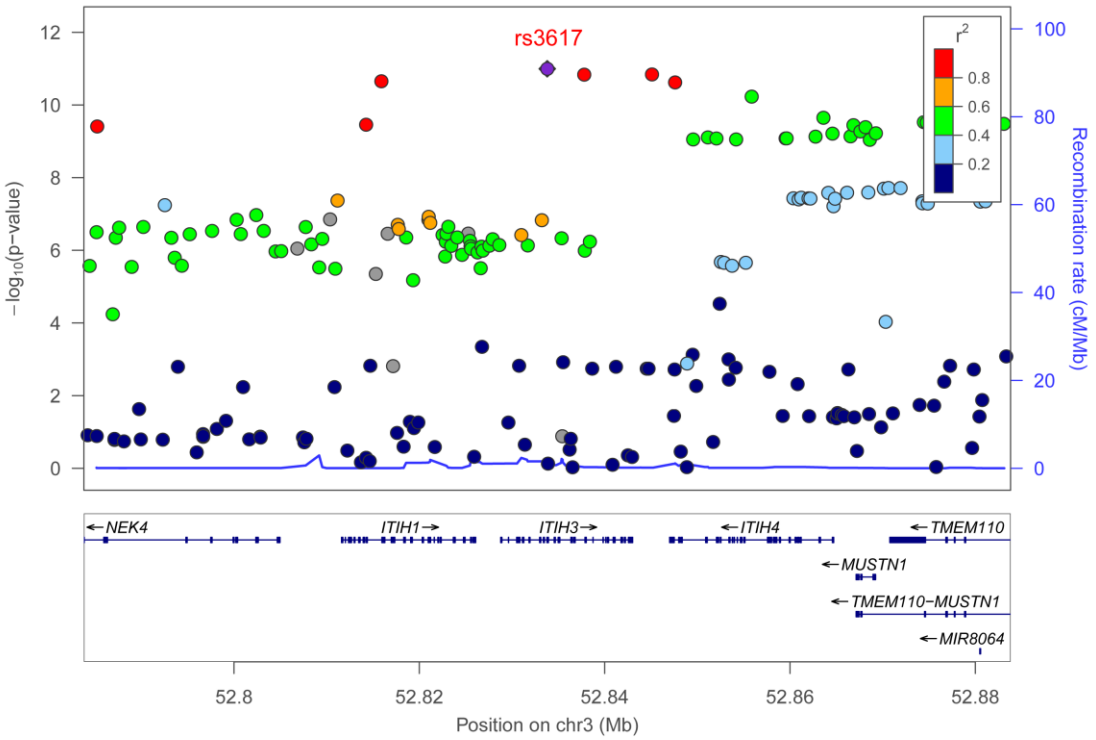

Fig. S12. The genomic location of rs3617. SNP rs3617 is located downstream of *ITIH4* gene. Of note, rs3617 was in high linkage disequilibrium (LD) with SNPs near *ITIH4* and *NEK4*. Data was from the study of Pardinas *et al* [2].

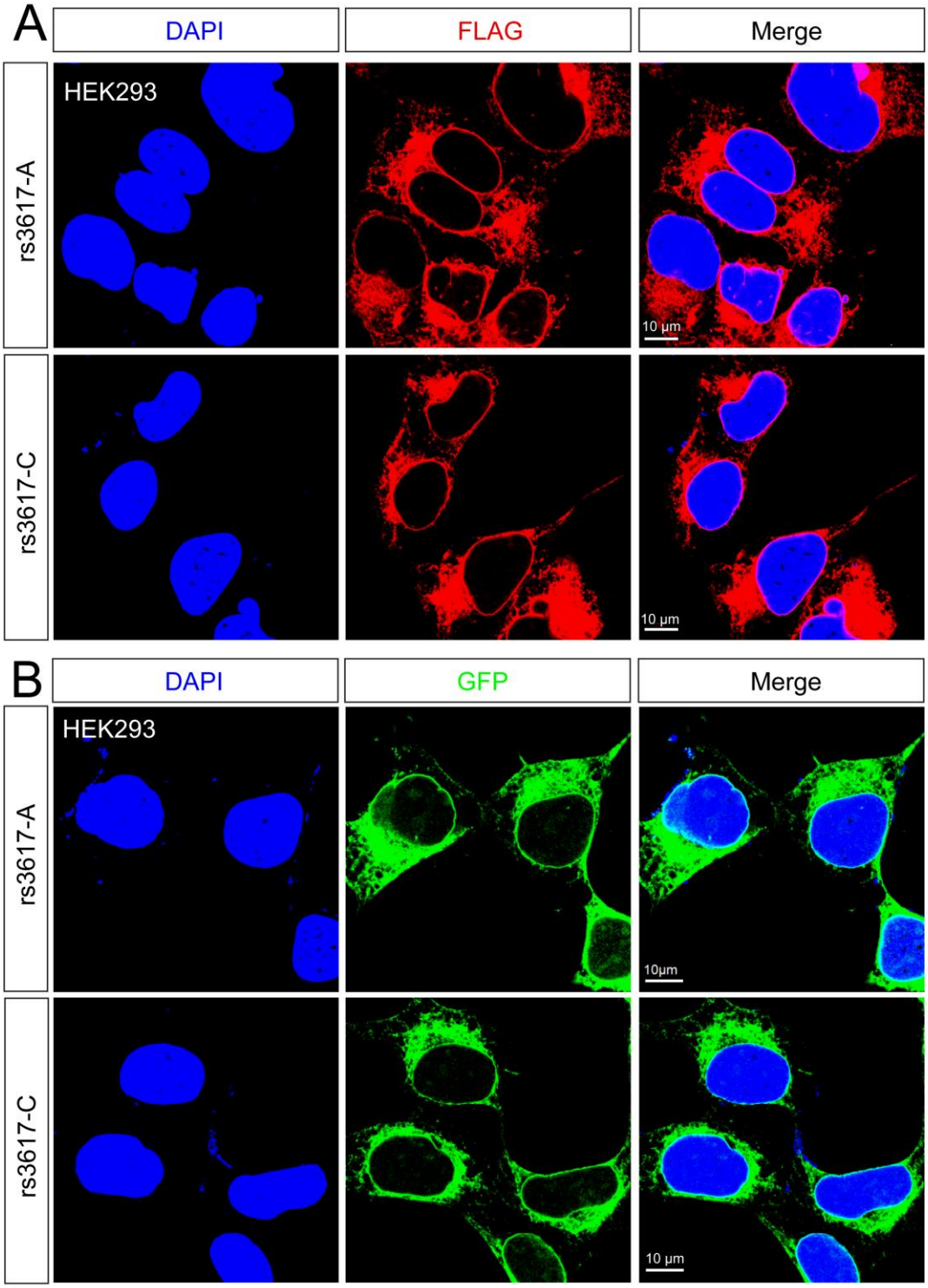

Fig. S13. SNP rs3617 did not affect subcellular localization of ITIH3 proteins. ITIH3 expression vectors containing different alleles of rs3617 were fused to FLAG or GFP. Immunofluorescence results indicated no obvious effect of different alleles of rs3617 on ITIH3 subcellular localization in HEK293 cells. Scale bar, 10 μm.

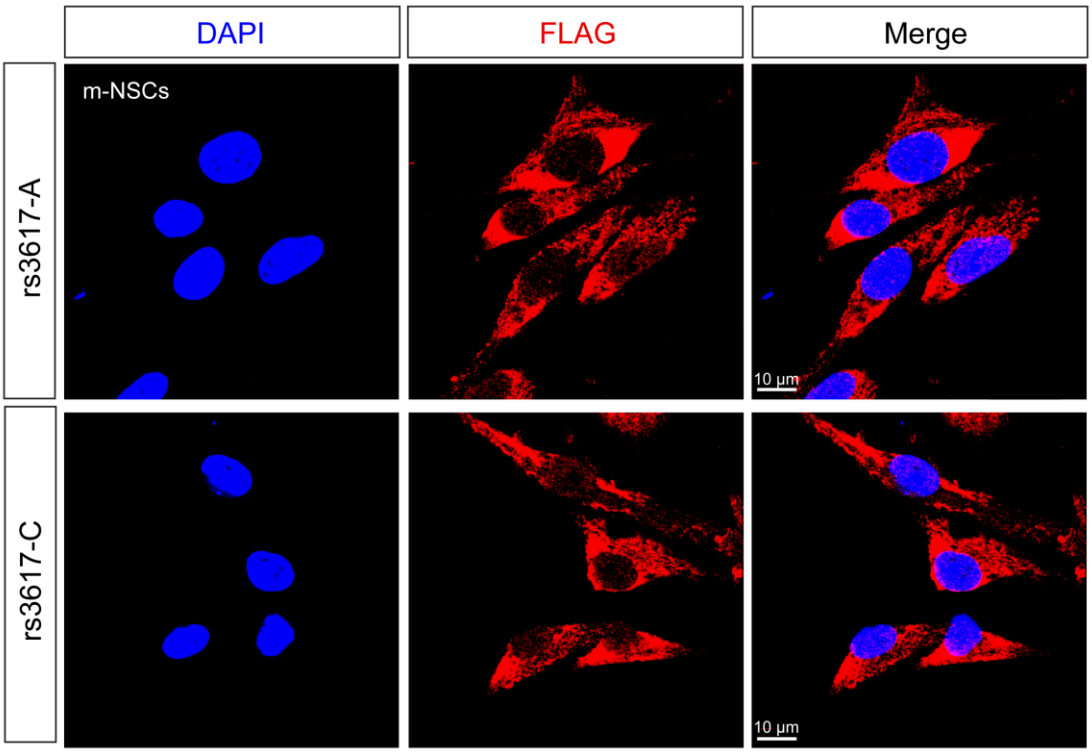

Fig. S14. SNP rs3617 did not affect subcellular localization of ITIH3 proteins in mouse neural stem cells (NSCs). Immunofluorescence results indicated no obvious effect of different alleles of rs3617 on ITIH3 subcellular localization in mouse NSCs. Scale bar, 10 μm.

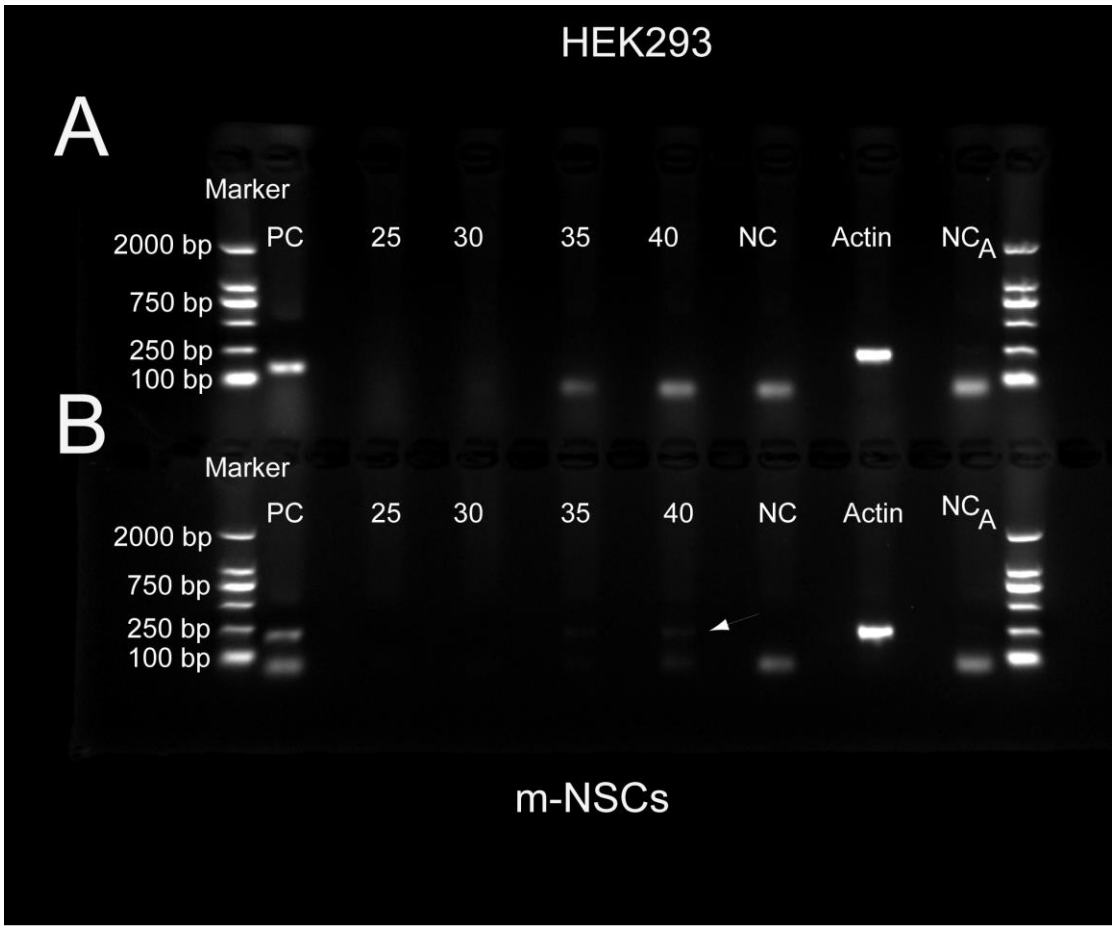

Fig. S15. RT-PCR showed no endogenous *ITIH3* expression in HEK293 cells and low *Itih3* expression in mouse neural stem cells. (**A**) In HEK293 cells, no endogenous *ITIH3* expression was detected. RNA extracted from HepG2 (which expresses *ITIH3*) were used as positive control and the length of PCR products of positive control was 149 bp. (**B**) In mouse neural stem cells, *Itih3* expression was very low. Arrowhead marks the endogenous *Itih3* expression in mouse neural stem cells. RNA extracted from mouse liver tissue were used as positive control the length of PCR products of positive control was 214 bp. PC, positive control; the numbers showed the PCR cycles used for RT-PCR; NC, negative control for *ITIH3*, NC_A, negative control for *Actin.*

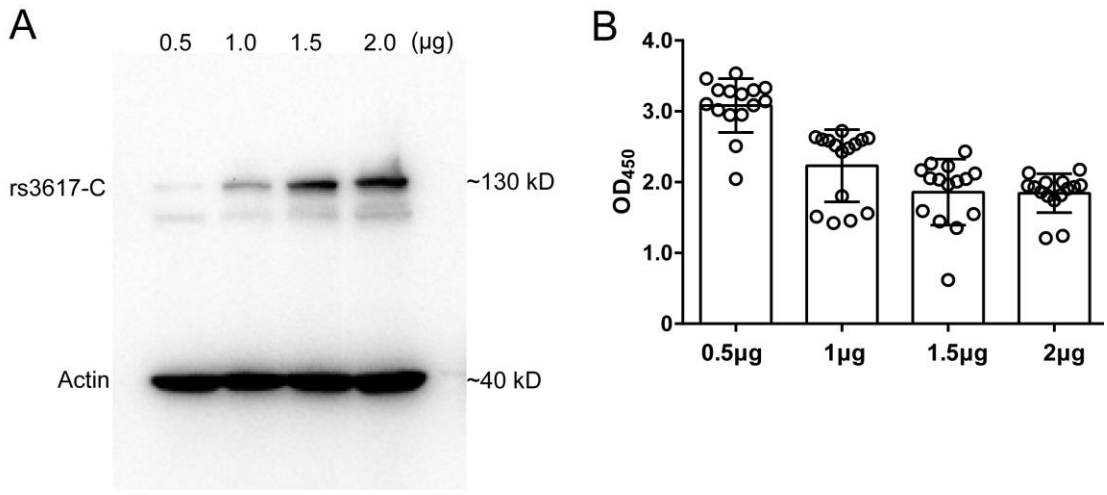

Fig. S16. Dosage-dependent effect of rs3617 on proliferation of HEK293 cells. (A) ITIH3 expression level was proportional to the amount of transfected ITIH3 expression vector. (**B**) The proliferation ability of HEK293 cells was decreased with the increase of transfected ITIH3 expression vector amount.

References

1. **Fagerberg L, Hallstrom BM, Oksvold P, Kampf C, Djureinovic D, Odeberg J, Habuka M, Tahmasebpoor S, Danielsson A, Edlund K, Asplund A, Sjostedt E, Lundberg E, Szigyarto CA, Skogs M, Takanen JO, Berling H, Tegel H, Mulder J, Nilsson P, Schwenk JM, Lindskog C, Danielsson F, Mardinoglu A, Sivertsson A, von Feilitzen K, Forsberg M, Zwahlen M, Olsson I, Navani S, Huss M, Nielsen J, Ponten F and Uhlen M. Analysis of the human tissue-specific expression by genome-wide integration of transcriptomics and antibody-based proteomics. Mol Cell Proteomics. 2019;13:397-406.**
2. **Pardinas AF, Holmans P, Pocklington AJ, Escott-Price V, Ripke S, Carrera N, Legge SE, Bishop S, Cameron D, Hamshere ML, Han J, Hubbard L, Lynham A, Mantripragada K, Rees E, MacCabe JH, McCarroll SA, Baune BT, Breen G, Byrne EM, Dannlowski U, Eley TC, Hayward C, Martin NG, McIntosh AM, Plomin R, Porteous DJ, Wray NR, Caballero A, Geschwind DH, Huckins LM, Ruderfer DM, Santiago E, Sklar P, Stahl EA, Won H, Agerbo E, Als TD, Andreassen OA, Baekvad-Hansen M, Mortensen PB, Pedersen CB, Borglum AD, Bybjerg-Grauholm J, Djurovic S, Durmishi N, Pedersen MG, Golimbet V, Grove J, Hougaard DM, Mattheisen M, Molden E, Mors O, Nordentoft M, Pejovic-Milovancevic M, Sigurdsson E, Silagadze T, Hansen CS, Stefansson K, Stefansson H, Steinberg S, Tosato S, Werge T, Collier DA, Rujescu D, Kirov G, Owen MJ, O'Donovan MC and Walters JTR. Common schizophrenia alleles are enriched in mutation-intolerant genes and in regions under strong background selection. Nat Genet. 2018;50:381-389.**